Friction and wear behaviour of Mo − W doped carbon-based coating during boundary lubricated sliding

HOVSEPIAN, Papken, MANDAL, Paranjayee, EHIASARIAN, Arutiun, SAFRAN, G, TIETEMA, Roel and DOERWALD, D

Published version

HOVSEPIAN, Papken, MANDAL, Paranjayee, EHIASARIAN, Arutiun, SAFRAN, G, TIETEMA, Roel and DOERWALD, D (2016). Friction and wear behaviour of Mo − W doped carbon-based coating during boundary lubricated sliding. Applied Surface Science, 366, 260-274.

Friction and wear behaviour of Mo − W doped carbon-based coating during boundary lubricated sliding

Papken Eh. Hovsepian[1], Paranjayee Mandal[1]*, Arutiun P. Ehiasarian[1], G. Sáfrán[2], R. Tietema[3], D. Doerwald[3]

[1)] Nanotechnology Centre for PVD Research, HIPIMS Research Centre, Sheffield Hallam University, City Campus, Howard Street, Sheffield S1 1WB, United Kingdom

[2)] Institute for Technical Physics and Materials Science, Centre for Energy Research, Hungarian Academy of Sciences, H-1121 Budapest, Konkoly-Thegeut 29-33 Hungary

[3)] IHI Hauzer Techno Coating B.V. Van Heemskerckweg 22, 5928 LL Venlo, The Netherlands

Email: p.hovsepian@shu.ac.uk, 200712mum@gmail.com, a.ehiasarian@shu.ac.uk, safran.gyorgy@ttk.mta.hu

Abstract

A molybdenum and tungsten doped carbon-based coating (Mo−W−C) was developed in order to provide low friction in boundary lubricated sliding condition at ambient and at high temperature. The Mo−W−C coating showed the lowest friction coefficient among a number of commercially available state-of-the-art DLC coatings at ambient temperature. At elevated temperature (200°C), Mo−W−C coating showed a significant reduction in friction coefficient with sliding distance in contrast to DLC coatings. Raman spectroscopy revealed the importance of combined Mo and W doping for achieving low friction at both ambient and high temperature. The significant decrease in friction and wear rate was attributed to the presence of graphitic carbon debris (from coating) and 'in-situ' formed metal sulphides (WS_2 and MoS_2, where metals were supplied from coating and sulphur from engine oil) in the transfer layer.

*Corresponding author email: 200712mum@gmail.com, Tel no: +44 0114 225 4081

1. Introduction

Metal-free and metal-doped diamond-like-carbon (DLC) coatings are extensively used as tribological coatings for engine parts due to their excellent combination of low friction and improved wear resistance properties. Engine components such as piston rings, piston pins, cam followers, cam shafts, rockers, gears and tappets are often coated with DLC and involve interfacial contacts with either steel or DLC coated surfaces in the presence of lubricant (formulated engine oil). But it is quite challenging to use DLC on the components, which are operated at high temperature and pressure conditions and at high sliding velocity (such as piston-cylinder and valve-train assembly, where maximum operating temperature typically is in the range of 300°C and 150°C respectively [1]).

It is well understood that DLC coatings show low friction and high wear resistance at ambient temperature due to formation of graphitic tribolayer at the asperity contacts [2], [3]. The tribological behaviour of these coatings however is strongly influenced by the operational environment. Hydrogenated DLC coatings for example show higher friction with increasing humidity whereas lower friction is observed for hydrogen-free DLC (a-C and ta-C) coatings due to termination of the dangling bonds. Moreover with increase of the test temperature (100°C – 300°C), both graphitisation and oxidation of DLC coating degrade the coating properties leading to a substantial increase in both friction and wear coefficients [4]. However DLC coating can survive comparatively higher temperature in the presence of lubricant, which isolates the coating from the hostile environment of the surroundings and acts as a coolant. The tribological performance at high temperature mostly depends on the test temperature, reactivity of the lubricant with the sliding surfaces (such as steel, DLC-coated, metal-doped DLC-coated etc), coating architecture and the coating deposition procedure. Therefore in high temperature applications (200°C and above), it is imperative that the coatings possesses qualities like high thermal stability, strong coating–substrate

adhesion, low coefficient of friction and high wear resistance. Furthermore it is important to understand that the coating and the surrounding ambient are two parts of one special tribo-system where the interplay between these two parts defines the overall tribological performance. Several approaches have been explored to achieve enhanced performance.

One such approach is the exploitation of the tribolayer formation process during lubricated sliding. It is well known that the tribological performance of the DLC coatings can be successfully manipulated by the chemistry of the lubricants used. For example, some of the state-of-the art formulated engine oils contain anti-wear (AW) additives such as Zinc dialkyl dithiophosphate (ZDDP), extreme-pressure (EP) additives and friction modifier such as Molybdenum dithiocarbamate (Mo-DTC). During sliding, Mo-DTC is thermally decomposed forming tribolayer containing both MoS_2 and MoO_3 [5], [6], [7], [8]. The friction is significantly reduced due to formation of MoS_2; however it has been shown that MoO_3 acts as a third body abrasive media, which increases the wear rate of the DLC coating [9]. An optimised concentration of ZDDP in the engine oil can promote the formation of MoS_2 over MoO_3 and reduce but not completely remove the negative effect of the MoO_3 [10], [11]. It is accepted in general that, formation of MoS_2-containing tribolayer reduces the friction when steel or DLC-coated surfaces are used as counterfaces.

When the engine oil is free of friction modifier, the MoS_2-containing tribolayer cannot be formed leading to higher friction coefficient. Fairly high friction coefficient (μ~0.1 – 0.3) was reported for amorphous DLC (a-C:H) coating in the temperature range of 20°C – 200°C, when lubricant was free from Mo-DTC but composed of base oil (such as polyalphaolefin or mineral oil) and additives (AW and EP) [12], [13]. Unlike amorphous DLC, significantly low friction coefficient is observed for tungsten-doped DLC coatings. Research showed that the chemical reactions occurring between the coating and the EP additives of the engine oil

produced WS_2-containing tribolayer. The WS_2 compound played the role of friction reducer due to its crystallographic structure. Formation of WS_2-containing tribolayer was well documented for W-DLC coatings during lubricated sliding at ambient temperature [14] as well as in the temperature range of 50°C – 200°C [13], [15], [16], [17], [18], [19]. For example, reactive magnetron sputtered WC-doped hydrogenated DLC coating (having multilayer structure of WC and a-C:H) showed $\mu \sim 0.055$ at ambient temperature due to formation of WS_2-containing tribolayer [14]. In another study, reactive magnetron sputtered W-DLC coating maintained similar friction coefficient ($\mu \sim 0.1 – 0.3$) in the temperature range of 50°C – 200°C due to formation of WS_2-containing tribolayer [13], [19], but it started to decompose at 200°C leading to high wear rate of the counterpart [13]. In all the cases discussed above, the formation of low-friction tribolayer during lubricated sliding plays an important, critical role for maintaining low coefficient of friction.

Another approach for further reduction of the friction is doping DLC with different metals. For example, the RF magnetron sputtered Ti-DLC and Mo-DLC coatings showed much lower friction ($\mu \sim 0.03$ and $\mu \sim 0.05 – 0.1$ respectively) compared to metal-free DLC coating ($\mu \sim 0.2$) when SAE 5W-20 formulated engine oil (contains polyalphaolefin, ZDDP and Mo-DTC) was used as lubricant. The low friction of Ti-DLC and Mo-DLC coatings was attributed to the formation of high strength metal carbides in the defective parts of the carbon network and formation of MoS_2-containing tribolayer due to thermal decomposition of Mo-DTC [20]. Similar to ambient temperature, formation of MoS_2-containing tribolayer in the temperature range of 50°C – 100°C decreases the friction ($\mu \sim 0.02 – 0.14$) of various metal-doped (such as Si-doped, Ti-doped and W-doped) DLC coatings under different test conditions [10], [21].

The addition of suitable doping elements into the DLC coating delays the graphitisation process and therefore is seen as a highly resourceful approach for preservation of coating properties to higher temperatures. It has been found that doping with Si, Mo or W increases the thermal stability of DLC coating up to ~500ºC [22], [23], [24], [25]. The formation of metal carbide phases during annealing stabilises the diamond-like structure and increases the thermal stability compared to metal-free DLC coating. Both the Mo-DLC and W-DLC coatings provide low friction at ambient condition. Depending on the presence of friction modifier in the lubricant, they are also able to provide reduced friction in elevated temperature.

However, with further increase in test temperature, (200°C and above) all the coatings discussed above significantly increase their friction and wear rate due to degradation of their properties. Therefore, these coatings cannot be classified as suitable for components used in high temperature applications and further research is needed to provide solution for this demand.

The aim of this research is to develop a new generation metal-doped carbon-based coating which is simultaneously doped with Mo and W. It is expected that the Mo − W doped carbon-based coating (Mo−W−C) will be able to produce "in-situ" a low-friction tribolayer during lubricated sliding via tribochemical reactive process taking place at the asperity contacts, which will allow operation at higher temperatures.

Further aim is to produce coating with highly dense microstructure and strong coating–substrate interfacial adhesion which will prevent coating delamination and therefore withstand more effectively wear during sliding. DLC research is well established and large number of vacuum based deposition techniques have been used over the years for the production of the various individual coatings belonging to this family. Most of these

techniques suffer from poor adhesion, lower density and high residual stress. We report first time the application of the High Power Impulse Magnetron Sputtering, (HIPIMS) as a technology for production of Mo-W doped carbon-based coatings. The high ionisation degree of the plasma generated in the HIPIMS discharge provides conditions for deposition of highly dense, strongly adherent and very smooth (low growth defect density) coatings [26], [27], [28] which is of paramount importance for any tribological coating. This study represents the most in-depth research so far in the understanding of microstructure formation and wear mechanism in the system.

2. Experimental details

2.1. Sample preparation and coating deposition

Prior to coating deposition, mirror polished (average R_a ~0.01 µm) M2 grade HSS disc samples (ø 30 mm × 6 mm) were cleaned in an industrial sized automated ultrasonic cleaning line using alkali water solutions to remove surface impurities and then dried in a high temperature vacuum drier before loading into the coating chamber. The Mo − W doped carbon-based coating (Mo−W−C) was deposited using combined HIPIMS and UBM techniques in an industrial sized Hauzer HTC 1000−4 PVD coating machine enabled with HIPIMS technology. A 200 nm thick base layer was deposited in reactive Ar + N_2 atmosphere in order to enhance the coating – substrate adhesion, followed by the deposition of ~2.2 µm thick Mo−W−C coating in non- reactive Ar atmosphere. The coating architecture consisted of a HIPIMS engineered interface, Mo − W − N base layer and a Mo − W − C top layer. The coating showed high adhesion with substrate (scratch adhesion test critical load L_c~80.8 N) and moderate hardness (~1677.5 HV). More details about the deposition of

Mo−W−C coating and the mechanical properties of the as-deposited coating were provided elsewhere [29].

The tribological properties of the Mo−W−C coating during boundary lubricated sliding at ambient temperature were compared with a range of commercially available state-of-the-art diamond-like carbon (DLC) coatings. The lowest friction coefficient was shown by $\mathrm{DLC(Cr/Cr\text{-}WC/W\text{:}C\text{-}H/a\text{:}C\text{-}H)}$ when compared to other DLC coatings namely DLC I, DLC II and DLC III. The $\mathrm{DLC(Cr/Cr\text{-}WC/W\text{:}C\text{-}H/a\text{:}C\text{-}H)}$ coating is a well-established state-of-the-art coating which has a special architecture containing a Cr base layer, followed by a sputtered Cr-WC adhesion layer, a W:C−H intermediate layer and an a:C−H top layer deposited by combined PVD and PACVD processes. Thus further on in this work, $\mathrm{DLC(Cr/Cr\text{-}WC/W\text{:}C\text{-}H/a\text{:}C\text{-}H)}$ coating was used as benchmark.

2.2. Characterisation techniques

The coatings architecture and microstructure were characterized by Transmission Electron Microscopy (TEM), Selected Area Electron Diffraction (SAED) and coupled analytical techniques. The TEM measurements were carried out by a 200kV PHILIPS CM 20 conventional TEM, equipped with a Brooker Si drift detector EDS and a 300kV JEOL 3010 High Resolution TEM (HRTEM) equipped with a GATAN Tridiem energy filter. Cross sectional samples for TEM investigations were prepared by conventional mechanical and ion beam thinning techniques.

CSEM room temperature and high temperature pin-on-disc tribometers were used to study the friction behaviour of Mo−W−C and state-of-the-art DLC coatings in boundary lubricated sliding condition. Commercially available engine oil Mobil1 Extended life^{TM} 10W-60 was used as lubricant and the tests were carried out at ambient (~30ºC and ~30% relative

humidity) and elevated (200ºC) temperatures. Both tribometers contained sample holder, which rotated against a stationary ball (used as a counterpart) under a static load. The coated disc and the counterpart were fully immersed into the oil during sliding. In this work, uncoated 100Cr6 steel balls and Al_2O_3 balls of 6 mm diameter were used as counterparts during sliding against coated HSS disc samples under static load of 5 N. The coefficient of friction $\mu = F_T / F_N$ was calculated during the experiment using a measured value for the tangential force F_T and a normal force F_N exerted by a calibrated weight. The wear coefficient was calculated using Archard's equation as $K_C = \frac{V}{F_N \times d}$ where V is the wear volume in m^3, F_N is the normal load in N and d is the sliding distance in meter. The volume of wear track (V) on the coated disc is calculated using the equation $V = 2\pi RA$, where R is the wear track radius and A is the cross-sectional area of the wear track. The area of the wear track profile was calculated by the software associated with the surface profilometer (DEKTAK 150). The scanning was repeated for 8 – 10 times on different sections of the wear track and the average was considered as area A, which was used in the equation mentioned above. The wear coefficients of the coatings and the counterparts were calculated with the help of an optical microscope.

Highly viscous Mobil1 Extended life™ 10W−60 synthetic engine oil was used as lubricant during sliding. The number '10W−60' indicates that the oil is multigrade, i.e. the oil has two viscosity grades '10W' and '60'. '10W' means it has same flowing characteristics as SAE 10 single-grade oil (typical viscosity ~4.1 centistokes) when starts from cold (W stands for Winter). '60' indicates that the oil is less thin than SAE 60 single-grade oil (typical viscosity ~24 centistokes) when temperature rises to 100ºC. This oil contains different polymer additives (mostly AW additives such as ZDDP and EP additives) but no friction modifiers (such as MoDTC). Sulphated ash (1.4 wt%) and phosphorus compounds (0.13 wt%) are the

main ingredients of this oil. Sulphated ash is composed of sulphur-based and chlorine-based compounds and different metal additives including K, Ba, Ca, Mg, Na and sometimes Sn and Zn. The metal additives are more reactive to phosphorus compounds compared to sulphur-based and chlorine-based compounds. Therefore, if the oil contains phosphorus compounds, the metal additives react with them under suitable conditions and produce metal phosphates and metal oxides (applicable for Sn and Zn only). Thus the sulphur-based and chlorine-based compounds become free to react chemically with other metals if present in the system depending on appropriate temperature and other operating conditions [30]. More details about the properties of this oil can be found elsewhere [31].

The tribological properties of Mo−W−C and $\mathrm{DLC}\left(\mathrm{Cr/Cr\text{-}WC/W:C\text{-}H/a:C\text{-}H}\right)$ coatings were investigated by analysing the wear tracks and the wear scar produced on the counterpart using optical and scanning electron microscopy (SEM), surface profilometer and Raman spectroscopy. The topographical imaging of the transfer layer formed on the ball surfaces and the wear tracks was carried out by secondary electron detector (ETD) of a fully computerised FEI NOVA NANOSEM 200 coupled with Energy Dispersive X-ray (EDX) analysis module (Oxford instruments X-max detector with INCA analysis software). X-ray mapping was done on the wear scar of the counterpart surfaces in order to identify the elemental composition of the adhered debris.

The Raman spectra were collected from the debris adhered to the counterpart surfaces and within the wear tracks after careful removal of the oil film using a Horiba-Jobin-Yvon LabRam HR800 integrated Raman spectrometer fitted with green laser (λ~532 nm). A 10% transmission filter was used to reduce the intensity of incident beam to avoid the damage due to irradiation. The samples were exposed to the laser for 60 seconds for spectrum collection and the collected spectra were averaged over 5 acquisitions in the wavelength range of 50 – 2250 cm^{-1}. During analysis, the background of spectrum was corrected using a 2^{nd} order

polynomial whereas a multi-peak Gaussian-fitting function was used to deconvolute the spectrum and identify the Raman peaks. More details on the parameters used during experiment and the spectrum analysis were described elsewhere [32]. To avoid ambiguity in peak position identification, powder samples from pure WS_2 and MoS_2 were analysed and their Raman spectra used as a reference.

3. Results and discussion

3.1 Coating phase composition and microstructure

Figures 1 (a and b) show the crystal structure of the as-deposited coating studied by XRD analysis using Bragg-Brentano and glancing angle (GAXRD) geometry respectively. The diffraction patterns in both geometries show broad peak between ~35.8° and ~38° and several sharp reflections belonging to the stainless steel substrate. The absence of the crystalline reflections and the broad diffuse peaks indicate that the film microstructure is essentially amorphous. The diffuse peak at 2θ ~35.8° corresponds to the hexagonal WC [100] and WN [100] phases and can originate from the main layer and the base layer of the film respectively. The peak at 2θ ~38° can be assigned to overlapping hexagonal W_2C [002] and Mo_2C [002] phases which most probably are present in the main coating. As no other peaks corresponding to these carbide phases are present, it is not possible to unambiguously state that the carbide phases have been formed. This concern is further strengthened by the relatively low deposition temperatures (below 400^{o}C), used during the coating growth.

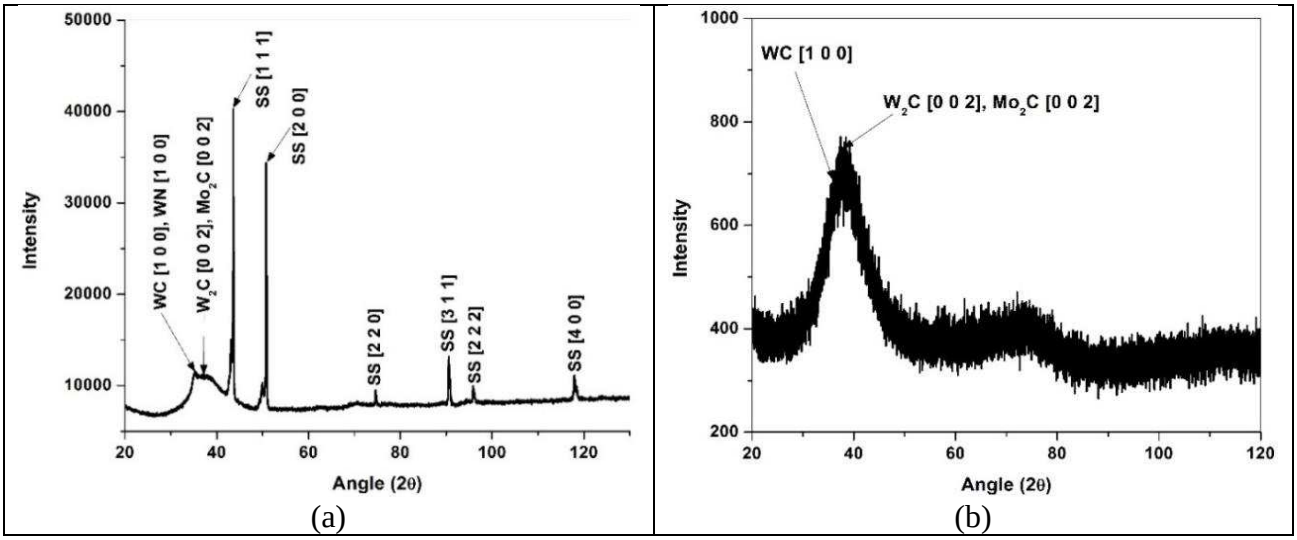

Figure 1: XRD spectra of the as-deposited coatings (a) Bragg-Brentano and (b) glancing angle geometry

Figures 2 (a and b) show the coating surface morphology and the fracture cross-section of the as-deposited Mo − W doped carbon-based coating respectively. The selected parameters during coating deposition provide dense columnar microstructure and a smooth surface with average surface roughness (R_a) in the order of 0.07 μm. The cross-sectional micrograph clearly reveals that the coating architecture consists of a thin Mo − W − N base layer (average thickness ~130 nm) adjacent to the Si substrate, which is followed by a thick (~2.2 μm) and dense columnar Mo − W − C layer on the top. Within the Mo − W − C layer , the column diameter is rather large, at approximately170 nm, and the columns are terminated with flat tops. This is often observed for high mobility and high irradiation growth which is typical for the HIPIMS deposition. Column boundaries are parallel to the growth direction of the film indicating no competitive growth.

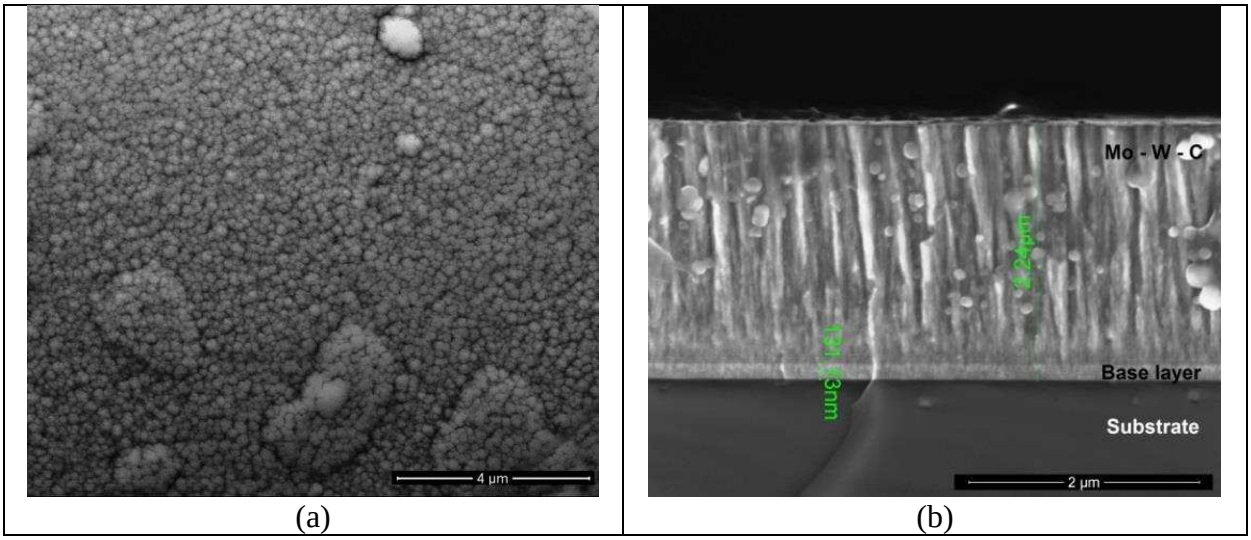

(a) (b)

Figure 2: (a) Surface morphology and (b) fracture cross-section SEM image of as-deposited Mo – W doped carbon-based coating

The cross sectional TEM investigation revealed further details of the Mo−W−C tribological coating architecture and structure. Low magnification image is shown in Figure 3 reveals extremely sharp and clean substrate-coating interface due to the HIPIMS etching [26], which explains the high coating adhesion (L_c~80.8 N). The base layer containing high amount of heavy elements such as W and Mo appears as a darker contrast ribbon with high density. The coating which is rich to light element, carbon appears as a brighter contrast layer. The main coating layer appears void-free, extremely dense which is attributed to the condensation of high energy particles generated in the HIPIMS discharge. Such particles possess enhanced surface mobility, promote the displacement of the atoms towards more stable position in terms of surface energy and result in elimination of voids, cavities, and vacancies in the coating. The selected area electron diffraction pattern (lower right inset) of the Mo−W−C layer shows strongly diffuse rings that indicate amorphous structure that was found all over the layer thickness thus confirming the findings of the XRD analyses.

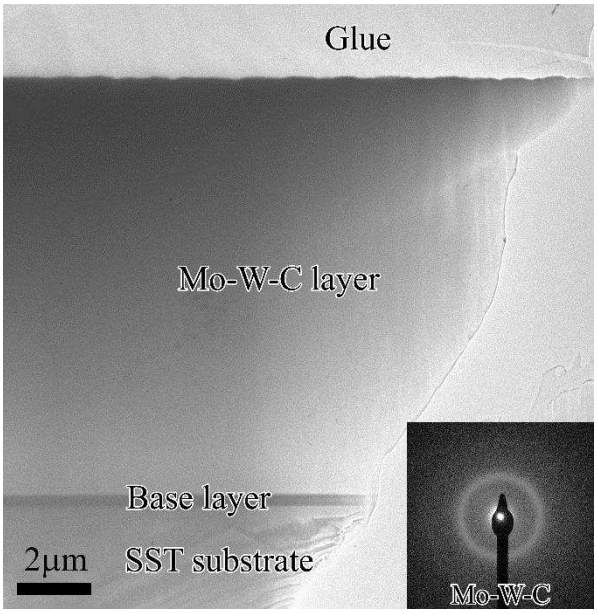

Figure 3: Low magnification TEM image showing the overall coating architecture. Inset: SAED pattern of the Mo-W-C layer

Higher magnification TEM images are shown in

Figure 4 from the bottom and top part of the coating respectively. The bottom part of the Mo−W−C coating contains a dense, layered structure, up to a couple of layers (a region ~ 100 nm thick), and the sub layers are undulated according to the top of the base layer, (see Figure 4a). SEM fracture cross-section (see Figure 2b) revealed a fine grained microstructure. The layering can be attributed to the specifics of the deposition process during the transition from base layer to the main layer. With increasing thickness, the main layer of the Mo−W−C coating developed to fibre-like that comprised a feather-like morphology, (Figure 4b). Formation of feather-like morphology is typical during growth in amorphous layers over thickness of several microns. A white contrast phase is accumulated at the columnar boundaries, which is believed to be pure carbon due to its high mobility and tendency for dynamic segregation during coating growth. Similar structures have been reported previously for C-Cr films deposited by magnetron sputtering in conditions of high ion irradiation [33], [34]. The segregation process is self-regulating and results from intense ion bombardment

which promotes diffusion of carbon atoms within the column. At the bias energies of this growth experiment, the diffusion is likely to be promoted within the top few monolayers of the coating. The presence of this phase may limit the diffusion of adatoms towards the column boundaries and arrest the lateral growth of the columns. This mechanism could explain the parallel inter-columnar boundaries observed in SEM cross sections (see Figure 2b).

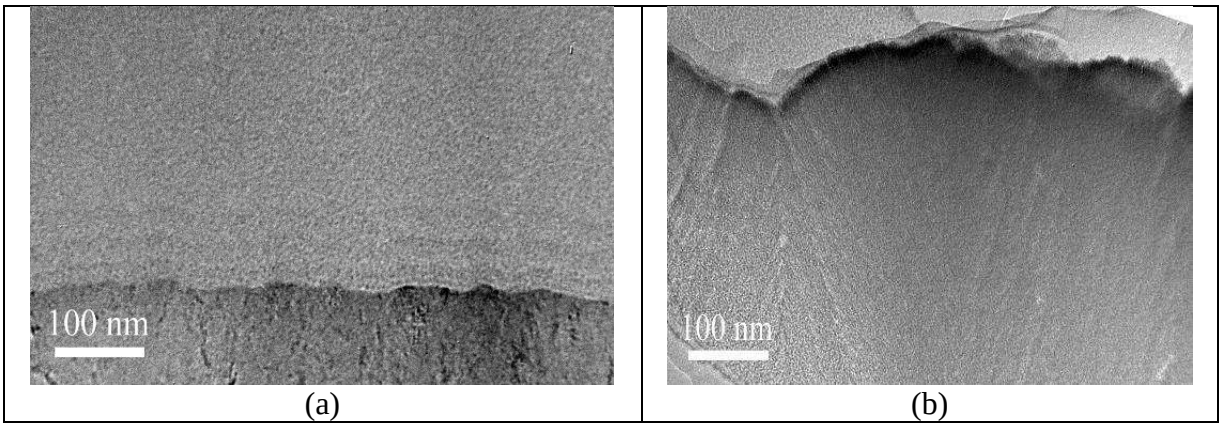

Figure 4: Higher magnification TEM images of (a) bottom part of the film and the underlying base layer, (b) top part of the film

3.2 Tribological behaviour of Mo-W-C and state-of-the-art DLC coatings at ambient temperature

3.2.1 Friction and wear behaviour

Figure 5 shows the friction behaviour of Mo−W−C and state-of-the-art DLC coatings against steel ball during lubricated sliding at ambient temperature (~30ºC and ~30% relative humidity). All the friction curves are observed to be very smooth throughout the sliding distance. The mean friction coefficients of state-of-the-art DLC coatings are observed in the range of $0.043 - 0.092$ with the lowest friction value achieved by DLC$\left(\text{Cr/Cr-WC/W:C-H/a:C-H}\right)$

coating. Further reduction in friction is observed for Mo−W−C coating with a mean friction coefficient of 0.033.

Figure 6 shows the wear track profile of Mo−W−C and DLC(Cr/Cr-WC/W:C-H/a:C-H) coatings after lubricated sliding and the images of the wear track are provided in the inset. DLC(Cr/Cr-WC/W:C-H/a:C-H) shows a shallow wear track with wear coefficient of 7.96×10^{-19} $m^3N^{-1}m^{-1}$, whereas no measurable wear is observed for Mo−W−C. The wear behaviour of both the coatings is further investigated using Raman spectroscopy.

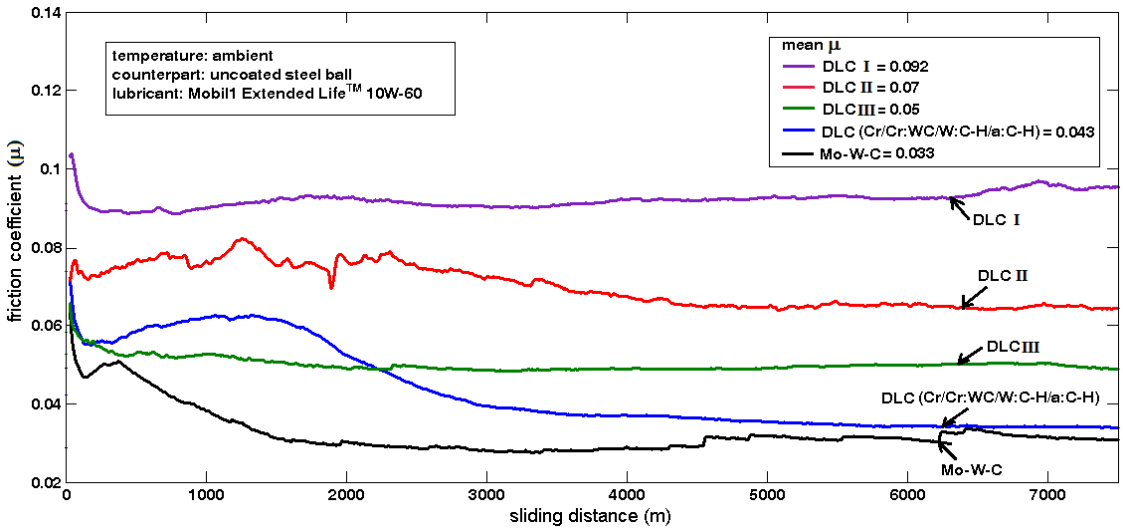

Figure 5: Friction behaviour of Mo−W−C and state-of-the-art DLC coatings during lubricated sliding against steel ball at ambient condition

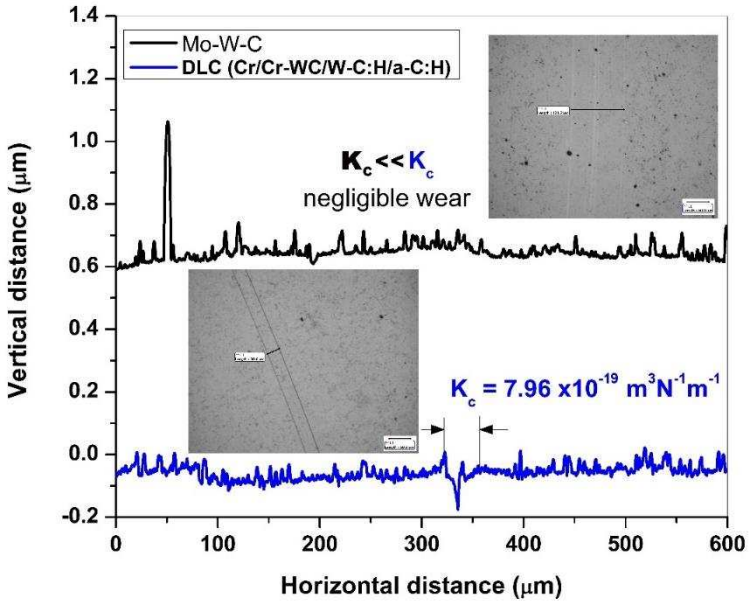

Figure 6: Wear track profiles of Mo−W−C and DLC(Cr/Cr-WC/W:C-H/a:C-H) coatings after lubricated sliding against steel ball at ambient temperature

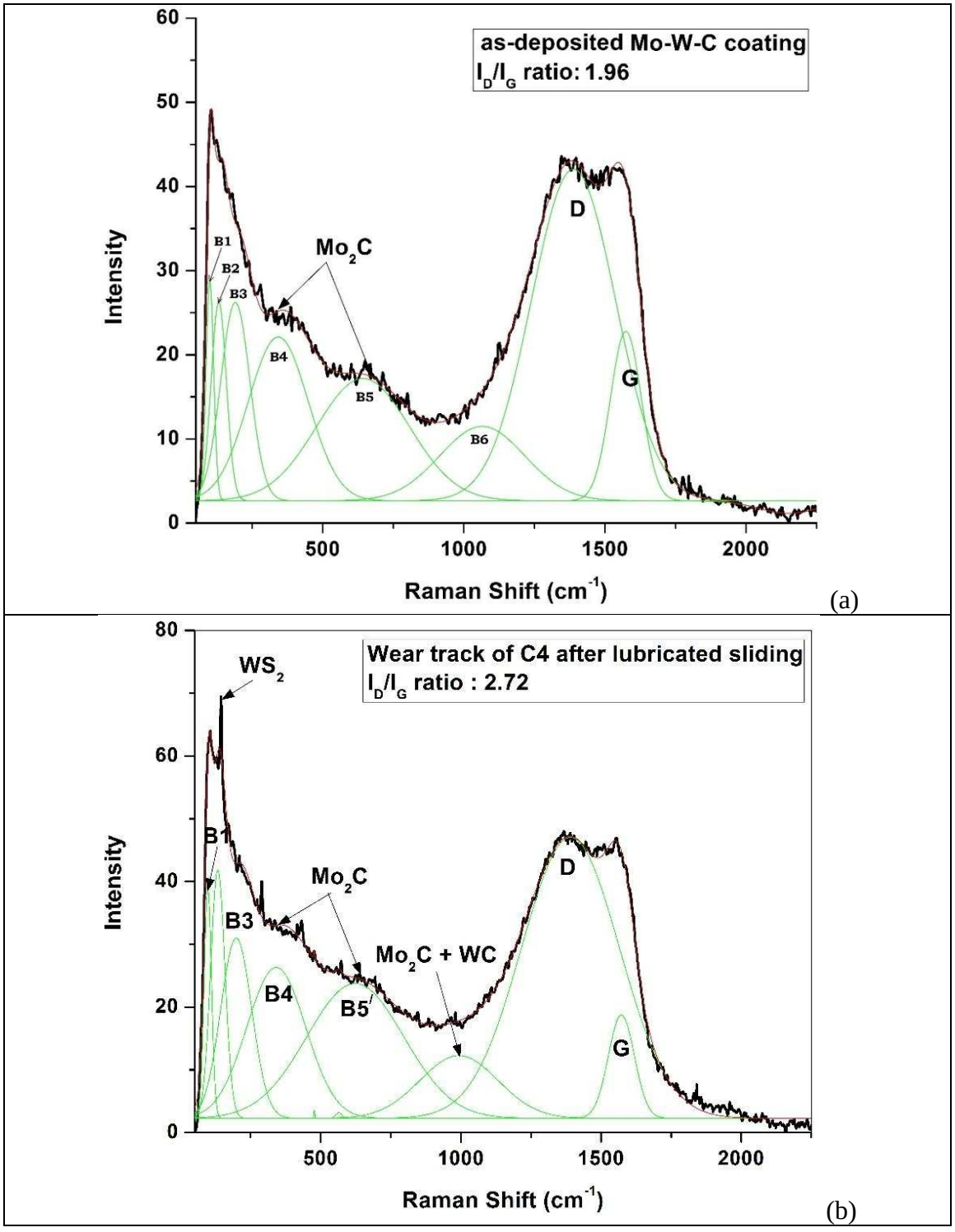

Figure 7a shows the Raman spectrum collected from as-deposited Mo−W−C coating. After deconvolution of the spectrum, the distinct and dominant disordered (D) and sp^2 bonded graphitic carbon peaks (G) are observed at 1387.04 cm^{-1} and 1574.32 cm^{-1} respectively. The I_D/I_G ratio is calculated as 1.96 indicating coating's graphitic nature. Except the graphitic peaks, all other deconvoluted peaks of as-deposited coating are listed in

Table 1. Among them, peaks B4 and B5 (centred at ~342 cm^{-1} and ~652 cm^{-1} respectively) are found at two consecutive shoulders of the spectrum and the corresponding peak widths are found as ~213 cm^{-1} and ~330 cm^{-1} respectively. These peaks belong to Mo_2C, because the dominant Raman peaks of commercial Mo_2C sample are observed at ~334 cm^{-1} and ~666 cm^{-1} [35].

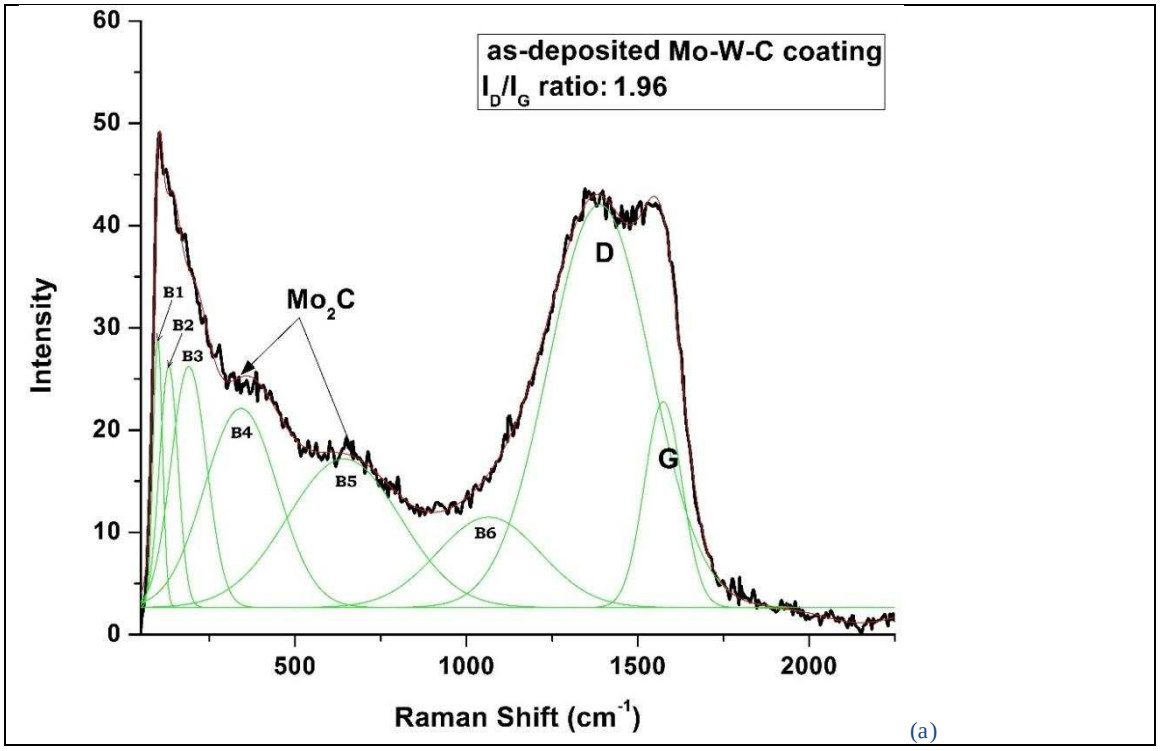

(a)

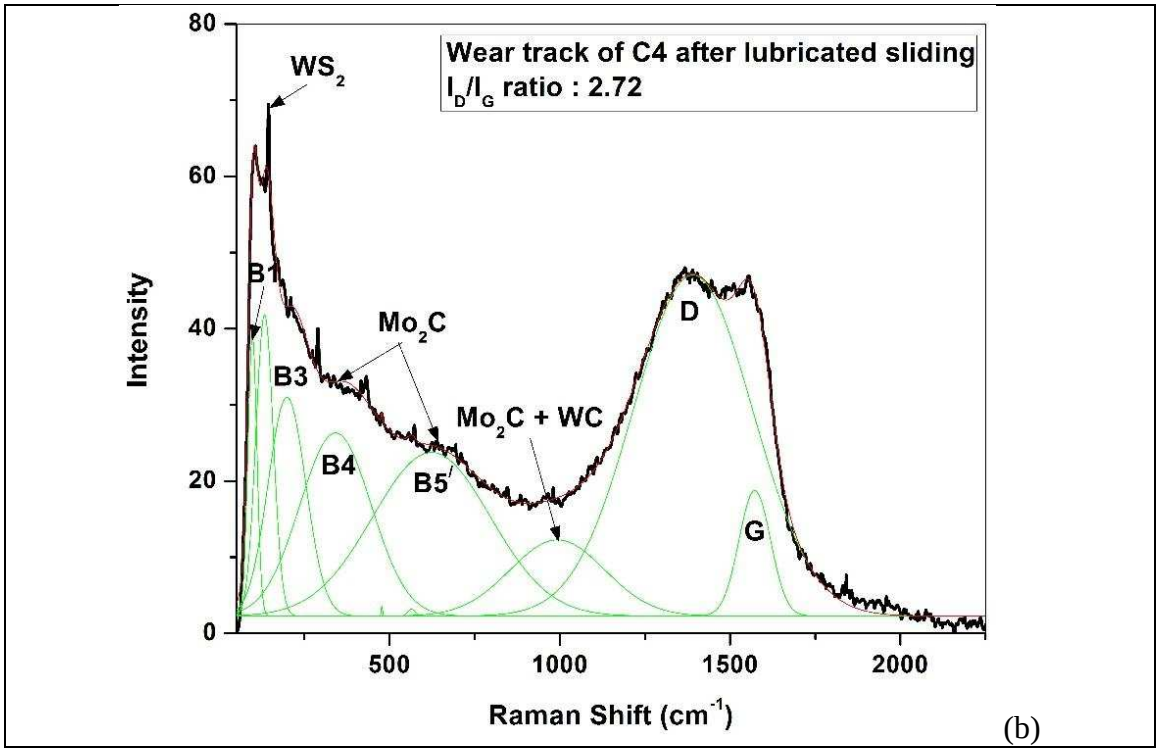

(b)

Figure 7b shows the spectrum collected within the wear track of Mo−W−C coating. After deconvolution of the spectrum, the D and G graphitic carbon peaks are found at 1390.85 cm^{-1} and 1572.61 cm^{-1} respectively and the I_D/I_G ratio is calculated as 2.72. The rest of the deconvoluted peaks are listed in Table 2. The I_D/I_G ratio is an important parameter in Raman analysis to understand the bonding characteristics and to estimate the disorder in the carbon network. The I_D indicates the intensity of D peak due to the A_{1g} breathing mode of carbon atoms in six fold rings. The I_G indicates the intensity of graphitic (G) peak resulting from the E_{2g} stretching motion for all pairs of sp^2 bonded carbon atoms. The as-deposited coating is graphitic, thus an increase in I_D/I_G ratio indicates an increase in disorder of carbon–carbon bonds in the coating after sliding. This increase in disorder in the carbon network helps to reduce the friction coefficient due to the irregularity of the bonds, which in turn weakens the material. The Mo_2C peaks (centred at ~341 cm^{-1} and at ~623 cm^{-1}) are observed within the shallow wear track similar to the as-deposited coating. The peak centred at ~993 cm^{-1} indicates possible overlapping of Mo_2C and WC phases as the leading Raman peaks of Mo_2C

and WC are reported in the literature at ~995 cm^{-1} [35] and ~960 cm^{-1} [36] respectively. The sharp peak centred at ~133 cm^{-1} is assigned to WS_2 as the leading Raman peak of WS_2 powdered sample used as a reference is observed ~128 cm^{-1} (see Figure 8a).

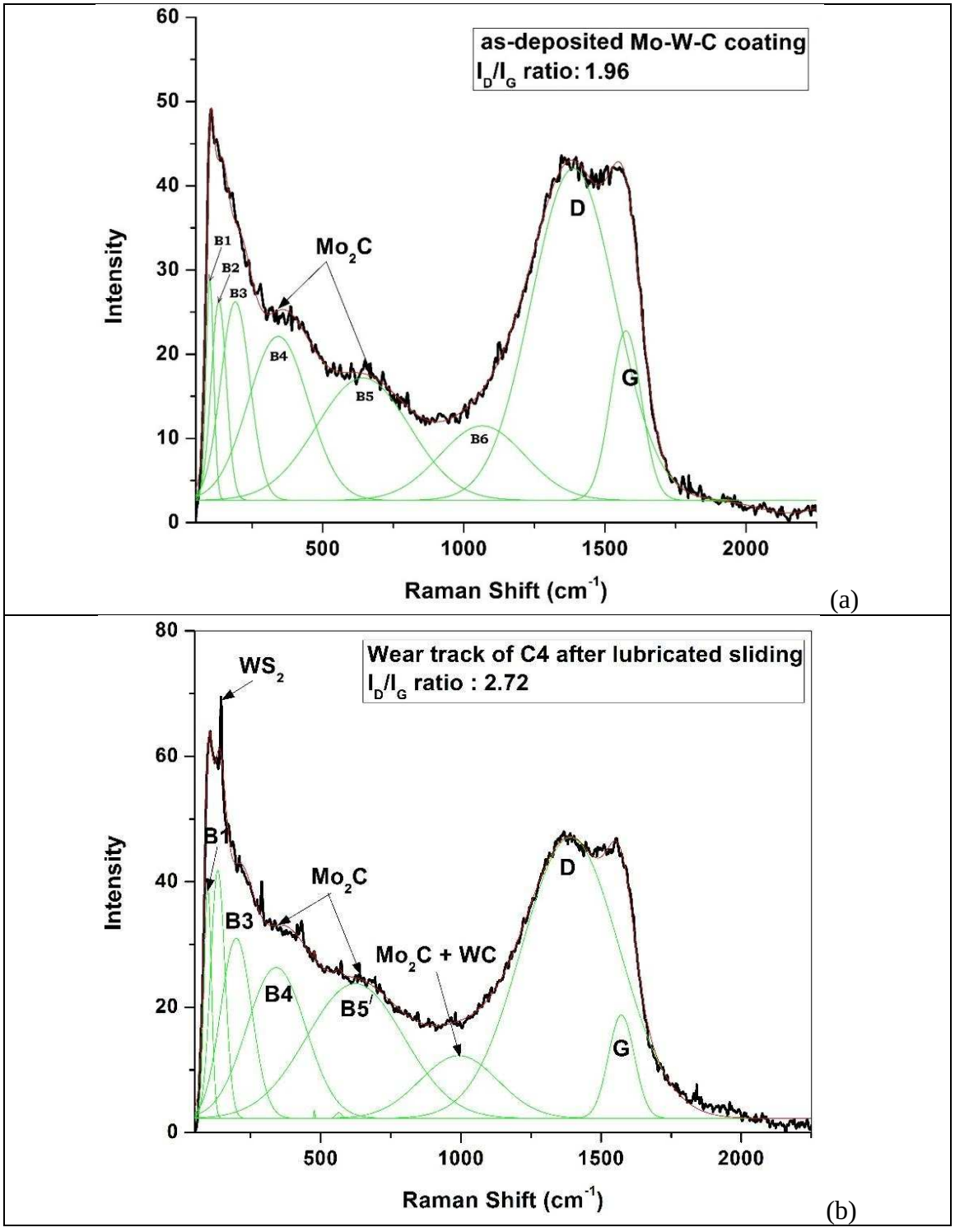

Figure 7: Raman spectra collected from (a) as-deposited Mo−W−C coating and (b) within the wear track after lubricated sliding at ambient temperature

Table 1: Raman peaks of the spectrum collected from as-deposited Mo−W−C coating

Raman peaks assigned to as-*deposited Mo−W−C*		Raman peaks (this work)	Raman peaks (literature)
B1		~ 100 cm^{-1} with a width of ~ 27 cm^{-1}	–
B2		~ 131.5 cm^{-1} with a width of ~ 54 cm^{-1}	
B3		~ 190 cm^{-1} with a width of ~ 103 cm^{-1}	
B4	Mo_2C	~ 342 cm^{-1} with a width of ~ 213 cm^{-1}	~334 cm^{-1} [35]
B5		~ 652 cm^{-1} with a width of ~ 330 cm^{-1}	~666 cm^{-1} [35]
B6		~ 1065 cm^{-1} with a width of ~ 302 cm^{-1}	–

Table 2: Raman peaks of the spectrum collected within the wear track of Mo−W−C coating after lubricated sliding against steel ball at ambient temperature

Raman peaks assigned to the wear track		Raman peaks (this work)	Raman peaks (literature)
B1		~ 97 cm^{-1} with a width of ~ 26 cm^{-1}	–
WS_2		~ 133 cm^{-1} with a width of ~ 51 cm^{-1}	~128 cm^{-1} [Figure 8a]
B3		~ 199 cm^{-1} with a width of ~ 111 cm^{-1}	–
B4	Mo_2C	~ 341 cm^{-1} with a width of ~ 210 cm^{-1}	~334 cm^{-1} [35]
B5/		~ 623 cm^{-1} with a width of ~ 346 cm^{-1}	~666 cm^{-1} [35]
Mo_2C		~ 993 cm^{-1} with a width of ~ 278 cm^{-1}	~995 cm^{-1} [35]
WC			~ 960 cm^{-1} [36]

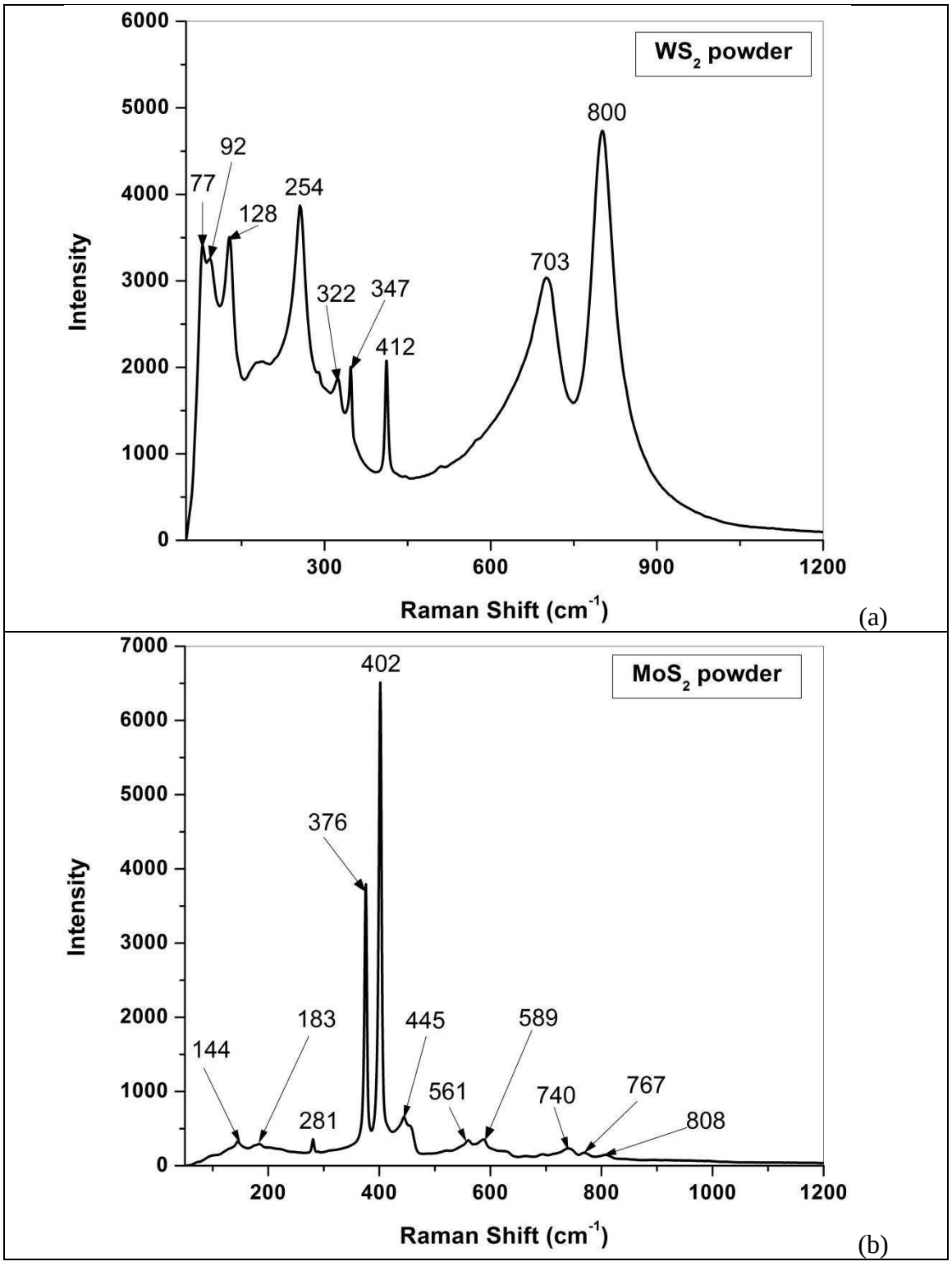

Figure 8: Raman spectra collected from (a) WS_2 and (b) MoS_2 powder

The Raman spectrum collected from as-deposited $DLC\left(Cr/Cr\text{-}WC/W\text{:}C\text{-}H/a\text{:}C\text{-}H\right)$ coating is shown in Figure 9a. The spectrum is dominated by G peak located at 1545.89 cm^{-1} because of its diamond-like structure and two separate disordered peaks (D1 and D2) are found at 1268.12 cm^{-1} and 1402.26 cm^{-1} respectively. The I_D/I_G ratio is found as 0.59. When Raman spectrum is collected from the wear track after lubricated sliding, the disordered (D1 and D2) and G peak positions are shifted towards higher wavenumbers as shown in Figure 9b. The D1, D2 and G peaks are found at 1301.5 cm^{-1}, 1481.4 cm^{-1} and 1558.93 cm^{-1} respectively and the I_D/I_G ratio increases to 1.14. The increase in I_D/I_G ratio and the dispersion of G peak position towards higher wavenumbers indicate the transformation of $DLC\left(Cr/Cr\text{-}WC/W\text{:}C\text{-}H/a\text{:}C\text{-}H\right)$ coating's diamond-like structure into graphite-like structure due to continuous rubbing action in between sliding surfaces.

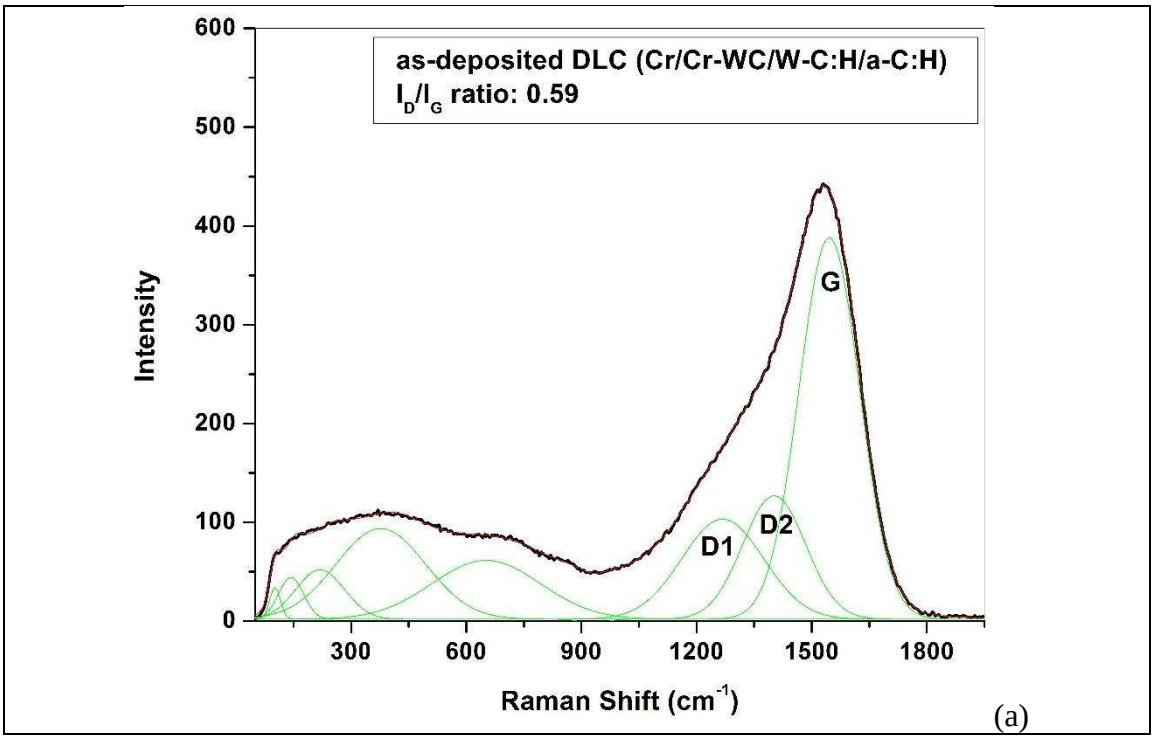

(a)

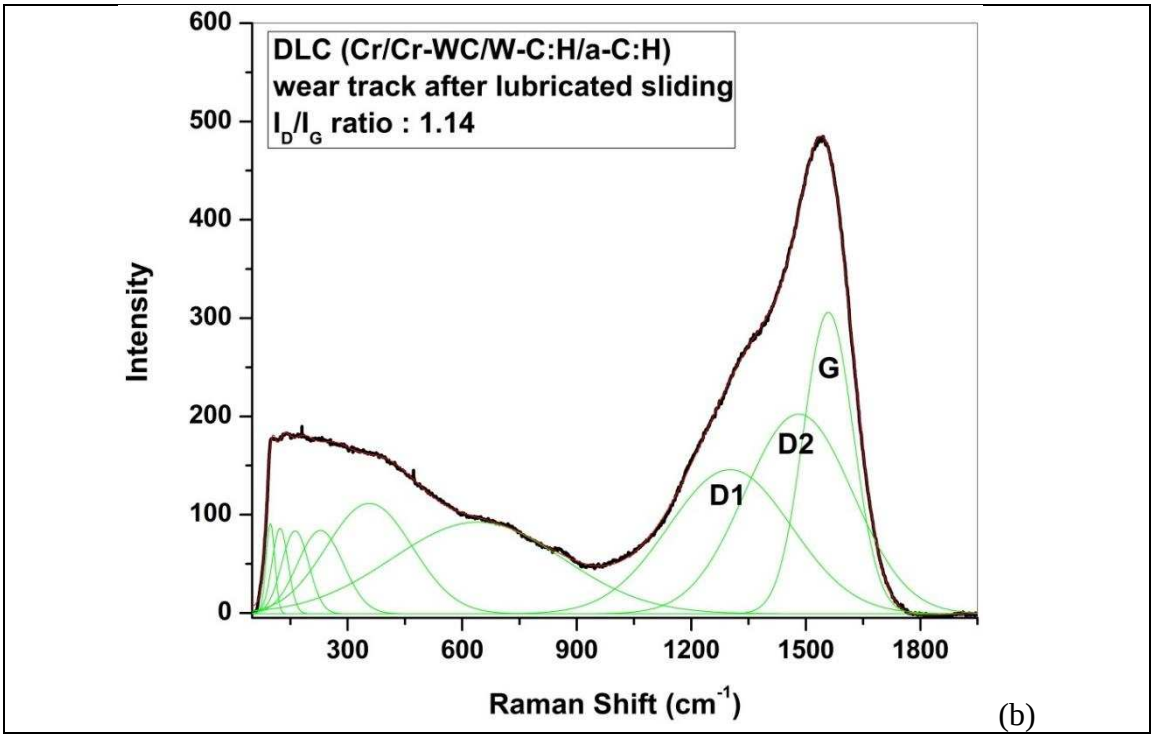

Figure 9: Raman spectra collected from (a) as-deposited DLC(Cr/Cr-WC/W:C-H/a:C-H) coating and (b) within the wear track after lubricated sliding at ambient temperature

3.2.2 Wear mechanism at ambient temperature

Raman analyses of the Mo−W−C coating reveal the wear mechanism during boundary lubricated sliding at ambient condition. Raman spectrum collected within the wear track indicates the presence of metal carbides (WC, Mo_2C etc.), metal sulphides (mostly WS_2) and graphitic carbon particles in the wear debris. The metal carbides and graphitic carbon particles belong to Mo−W−C coating, whereas WS_2 is a reaction product formed during lubricated sliding. During the continuous rubbing action between the coating and the counterpart the surface asperities get in frequent contacts generating high flash temperatures which trigger tribo-chemical reactions. In these conditions, the sulphur-containing compounds of the lubricant react with the material of the sliding surfaces resulting in "in-situ", formation of WS_2, where W comes from the Mo−W−C coating and S comes from the EP additives present in the engine oil and the engine oil itself. The sharp WS_2 peak observed in the Raman spectrum shows formation of significant amount of the lubricious WS_2

compound within the wear track due to the long sliding distance (i.e. 7.5 km). These analysis support the conclusion that the wear mechanism of Mo−W−C coating during boundary lubricated sliding is tribo-chemically reactive at ambient temperature.

WS_2 is a well-known solid lubricant. The structure consists of layers in which tungsten atoms are linked with six sulphides and form a trigonal prism rather than the usual octahedron structure. The layered structure promotes easy slipping between the layers and provides graphite-like lubricating properties [37]. MoS_2 is likely to be formed during lubricated sliding, however it cannot be detected using Raman analyses probably due to its small amount. The friction is further benefitted by the presence of graphitic carbon particles in the tribolayer. These debris particles adhere to the wear track by forming a thin tribo-layer, which promotes sliding and improves wear resistance. As a result, Mo−W−C coating shows low friction coefficient (μ= 0.033) and no measurable wear during lubricated sliding. Similarly negligible wear is observed on ball surface after sliding.

Unlike Mo−W−C coating, no tribochemically reactive wear mechanism is observed for $DLC\left(Cr/Cr\text{-}WC/W\text{:}C\text{-}H/a\text{:}C\text{-}H\right)$ coating at ambient condition. Raman analyses confirm no reaction between $DLC\left(Cr/Cr\text{-}WC/W\text{:}C\text{-}H/a\text{:}C\text{-}H\right)$ coating and engine oil during lubricated sliding. Thus the low friction and wear coefficients (μ=0.043 and $K_c \sim 10^{-19}$ $m^3N^{-1}m^{-1}$) of $DLC\left(Cr/Cr\text{-}WC/W\text{:}C\text{-}H/a\text{:}C\text{-}H\right)$ coating are attributed to its extremely high highness (>4300 HV) and the formation of tribolayer containing graphitic particles.

3.3 Tribological behaviour of Mo-W-C and state-of-the-art DLC coatings at 200ºC

3.3.1 Friction and wear behaviour against steel counterpart

Figure 10 shows the friction curves of Mo−W−C and $DLC\left(Cr/Cr\text{-}WC/W\text{:}C\text{-}H/a\text{:}C\text{-}H\right)$ coatings against steel counterparts at 200ºC. The friction curve of $DLC\left(Cr/Cr\text{-}WC/W\text{:}C\text{-}H/a\text{:}C\text{-}H\right)$ shows

a rapid decrease in friction in "run-in" period (segment I), followed by an increase in friction from middle of the segment II to the end of segment III. The mean friction coefficients are observed as ~0.056, ~0.048 and ~0.075 in segments I, II and III respectively. Analytical techniques confirm that the wear debris produced from the DLC(Cr/Cr-WC/W:C-H/a:C-H) coating is of graphitic nature, (see Figure 15b), which explains the decrease in friction coefficient in "run-in" period. However degradation of coating properties at 200ºC increases the friction coefficient later (see segment III). On the other hand, Mo−W−C coating shows a high friction coefficient (μ~0.092) in "run-in" period (segment I), followed by a slow but steady decrease for rest of the sliding distance (see μ~0.068 and μ~0.056 in segments II and III respectively). This reduction in friction coefficient is attributed to the formation of the lubricious MoS_2 and WS_2 during sliding (see Figure 11, Figure 12 and Figure 13b) as revealed by the X-ray mapping and Raman analyses. Scanning electron microscopy combined with Raman spectroscopy reveal further details of the wear behaviour of these coatings and the counterparts during lubricated sliding at 200ºC as explained in the following sections A and B.

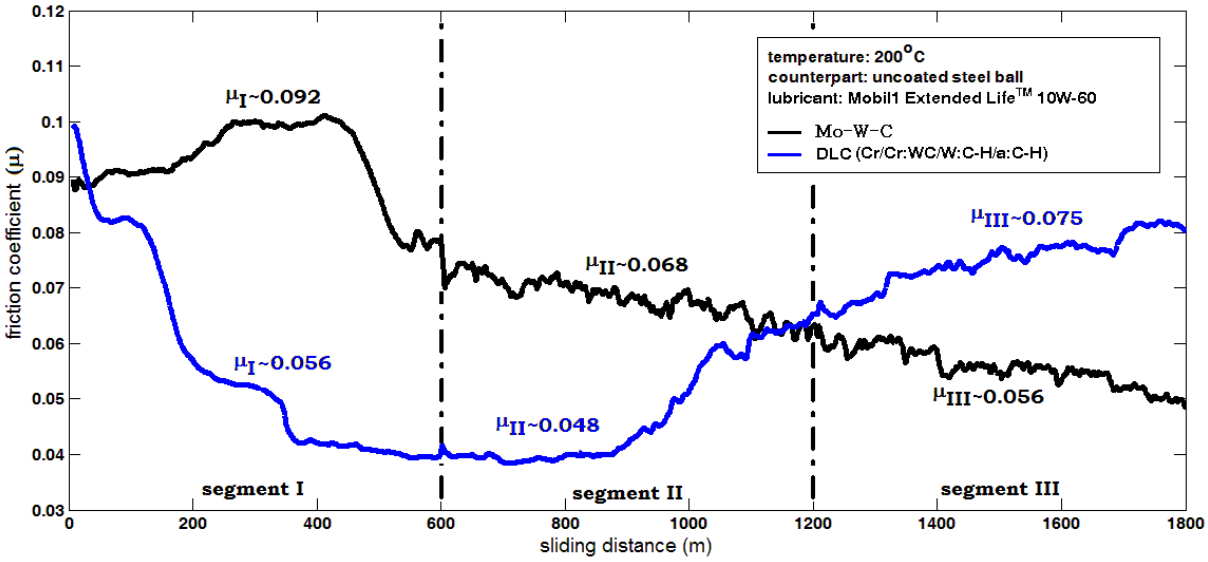

Figure 10: Friction behaviour of Mo−W−C and DLC(Cr/Cr-WC/W:C-H/a:C-H) coatings after lubricated sliding against steel ball at 200ºC

A. Analyses of the wear behaviour of Mo–W–C coating sliding against steel counterpart

Figure 11a shows the SEM images and the EDX analyses of the debris adhered to the steel ball after lubricated sliding against Mo−W−C coating at 200ºC. The first image shows an overall view of the debris adhered to the steel ball surface and two further images of the debris are taken at lower and higher magnifications. Based on the area of the wear scar observed in the SEM image, the wear coefficient of the steel ball was calculated as 3.44×10^{-13} $m^3N^{-1}m^{-1}$. Further, the image taken at largest magnification clearly points out position **a**, where the debris is smeared on the ball surface and position **b**, where the debris is accumulated and thickened on the ball surface. The EDX analysis is carried out on these two positions in order to reveal the elemental composition of the adhered debris. The EDX spectrum collected from position **a** shows strong peaks of Fe, Cr and C and weak peaks of W and S. Thus position **a** basically indicates the ball surface, which is possibly covered by graphitic carbon and WS_2 particles formed during sliding. The EDX spectrum collected from position **b** however, shows strong presence of W, Mo and S, which indicates that the accumulated debris on position **b** is a thick layer possibly consisted of a mixture of WS_2 and MoS_2. It is believed that both WS_2 and MoS_2 are formed due to the chemical reactions taking place at the asperity contacts during lubricated sliding and adhered to the ball surface. These solid lubricants significantly modify, reduce the friction coefficient during sliding at 200ºC.

Figure 11b shows the SEM image of the wear scar and the debris adhered to the steel counterpart after sliding against Mo−W−C coating and the X-ray maps of the elements present in the debris. The tungsten (W), molybdenum (Mo) and sulphur (S) maps show their presence only on the adhered debris. Carbon (C) and iron (Fe) are present all over the wear scar, however the intensity of iron is observed lower within the adhered debris areas. These

maps indicate that the adhered debris is a relatively thick layer composed mainly of graphitic carbon particles and sulphides of tungsten and molybdenum.

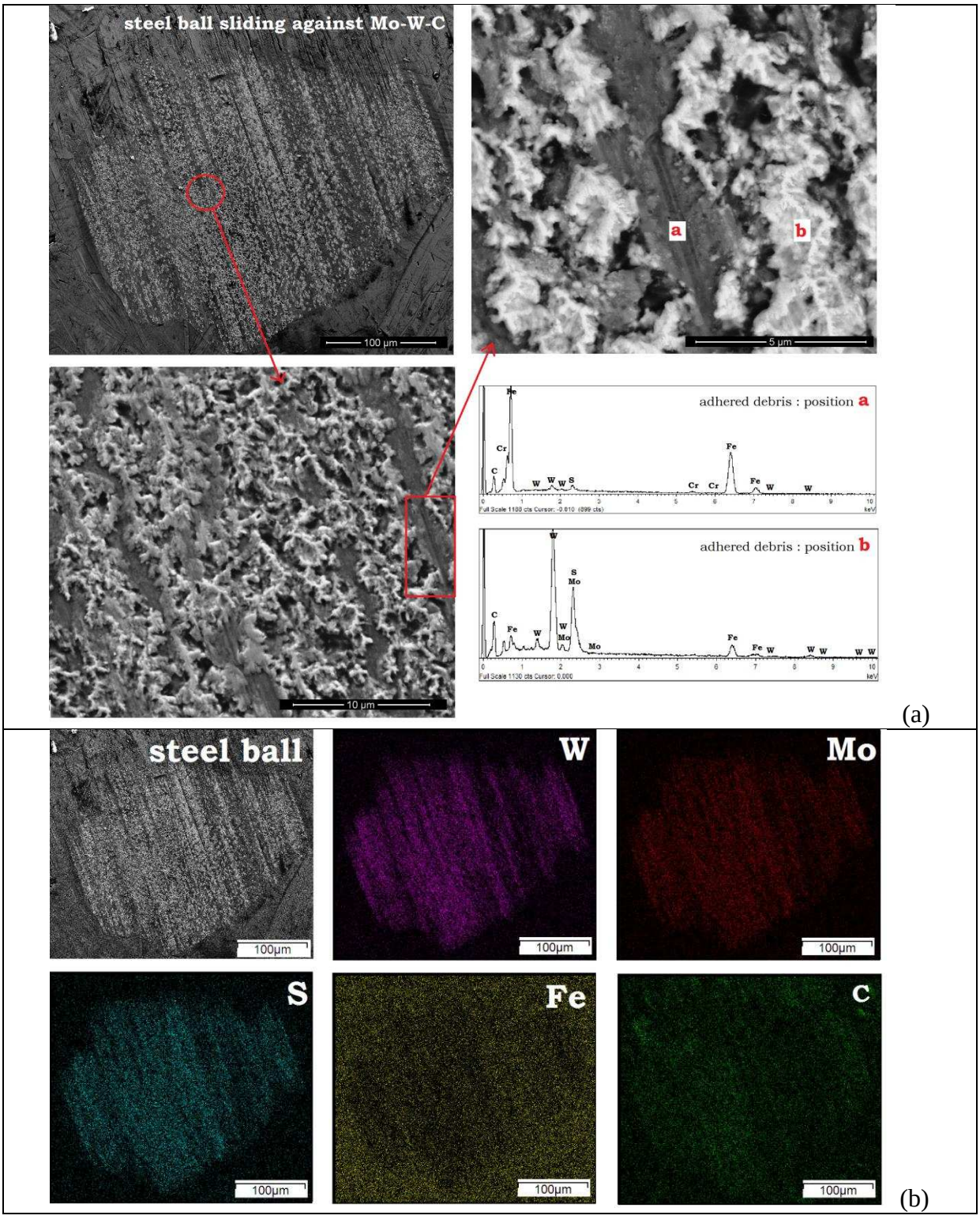

Figure 11: (a) Overall view of the warn surface of the steel ball counterpart, low and high magnification SEM images and EDX analyses results (patterns) and the (b) X-ray mapping of

the debris adhered to the steel counterpart after lubricated sliding against Mo−W−C coating at 200ºC

Figure 12 shows the Raman spectra collected from position **a** and position **b** of the adhered debris. The deconvoluted spectrum collected from position **a** (see Figure 12a) contains two separate disordered peaks (D1 and D2) and G peak located at ~1349.53 cm^{-1}, ~1479.81 cm^{-1} and ~1580.27 cm^{-1} respectively. The I_D/I_G ratio is calculated as 1.41. Among rest of the peaks, peaks P1 – P3/ belong to the steel ball, whereas peak centred at ~323 cm^{-1} indicates strong presence of WS_2 phase (Raman peak of WS_2 powdered sample is observed ~322 cm^{-1}, see Figure 8a) as listed in Table 3. These results support the findings of EDX analysis that position **a** on the ball surface is covered by graphitic carbon and WS_2 particles. On the other hand, two sharp peaks are observed centred at ~406.5 cm^{-1} and ~379 cm^{-1} respectively after deconvolution of the Raman spectrum collected from position **b** of the adhered debris (see Figure 12b). The dominant Raman peaks of WS_2 and MoS_2 powdered samples used as a reference are found ~412 cm^{-1} (see Figure 8a) and ~402 cm^{-1} (see Figure 8b) respectively, thus the highest peak in the Raman spectrum (centred at ~406.5 cm^{-1} with a width of ~9 cm^{-1}) belongs to WS_2 and MoS_2 phases. The second highest peak (centred at ~379 cm^{-1} with a width of ~12 cm^{-1}) belongs to MoS_2, as the leading Raman peak of MoS_2 powdered sample is observed ~376 cm^{-1} (see Figure 8b). These analyses provide evidence that the MoS_2 and WS_2 phases are "in-situ" formed during sliding due to tribochemical reactions occurred between Mo−W−C coating and the sulphur from the EP additives and the engine oil. Compared to the room temperature sliding, the rate of the chemical reactions are increased at 200ºC, thus more amount of metal sulphides are formed as indicated by the higher intensity peaks in the Raman spectra. Moreover, peaks P1 – P4 (see Figure 12b) belong to the steel ball as listed in Table 3. Therefore the Raman analyses completely agree with the findings of X-ray mapping and EDX analyses confirming presence of graphitic carbon particles and solid lubricants (WS_2 and MoS_2) in the adhered debris.

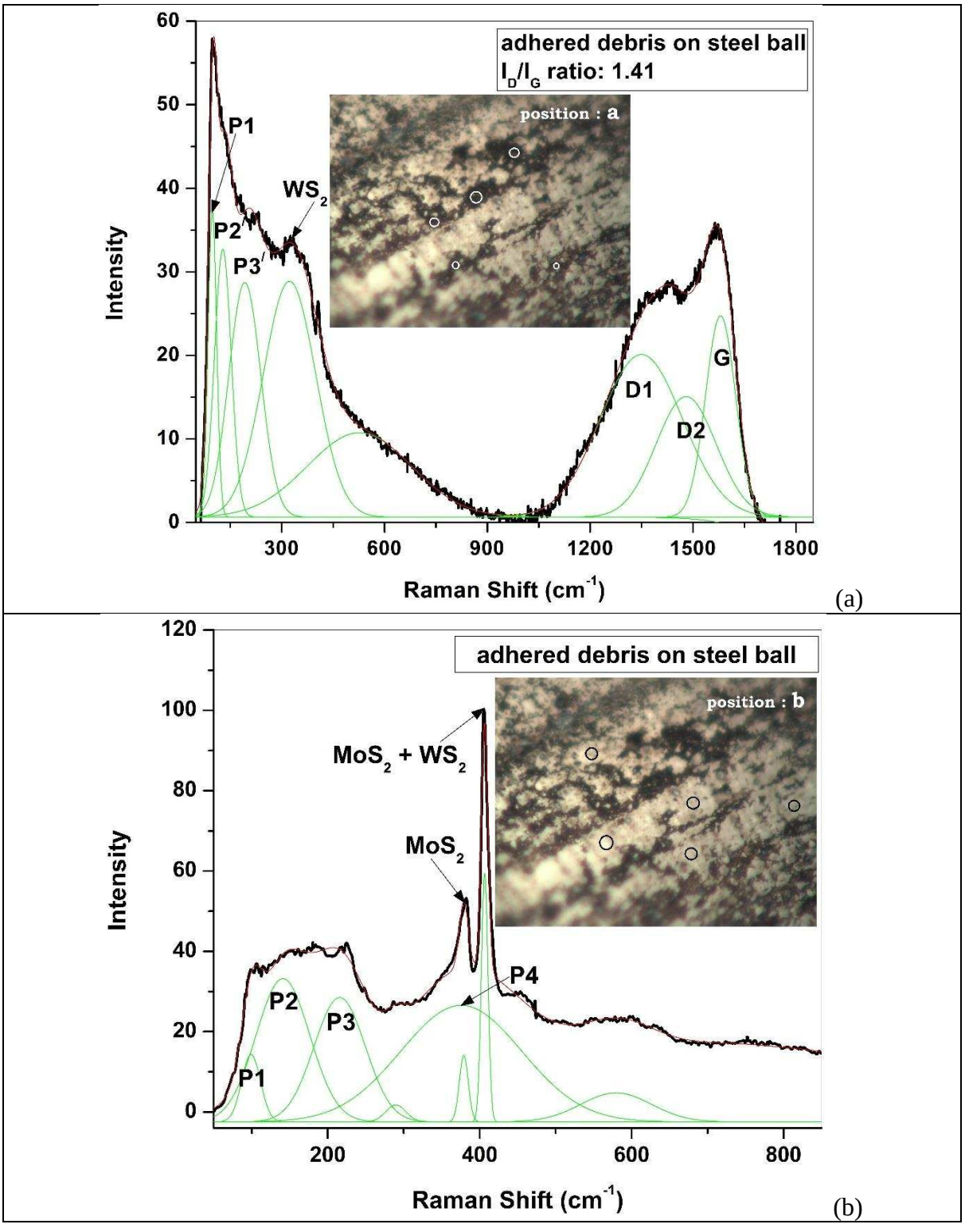

Figure 12: (a – b) Raman spectra collected from the debris adhered to the steel counterpart after lubricated sliding against Mo−W−C coating at 200ºC

Table 3: Raman peaks of the spectrum collected from the debris adhered to the steel ball after lubricated sliding against Mo−W−C coating at 200ºC

Raman peaks assigned to the adhered debris	Raman peaks (this work)	Raman peaks (literature)
(a) position 'a'		
P1	~ 98 cm^{-1} with a width of ~ 25 cm^{-1}	–
P2/	~ 128 cm^{-1} with a width of ~ 49 cm^{-1}	
P3/	~ 192 cm^{-1} with a width of ~ 93 cm^{-1}	
WS_2	~ 323 cm^{-1} with a width of ~ 153 cm^{-1}	~322 cm^{-1} [Figure 8a]
(b) position 'b'		
P1	~ 99 cm^{-1} with a width of ~ 25 cm^{-1}	–
P2	~ 141 cm^{-1} with a width of ~ 71 cm^{-1}	
P3	~ 216 cm^{-1} with a width of ~ 68 cm^{-1}	
P4	~ 376 cm^{-1} with a width of ~ 159 cm^{-1}	
MoS_2	~ 379 cm^{-1} with a width of ~ 12 cm^{-1}	~376 cm^{-1} [Figure 8b]
MoS_2	~ 406.5 cm^{-1} with a width of ~ 9 cm^{-1}	~402 cm^{-1} [Figure 8b]
WS_2		~412 cm^{-1} [Figure 8a]

Figure 13a shows the wear track profile of Mo−W−C coating after lubricated sliding against steel ball at 200ºC. The wear coefficient is calculated as ~1.11 × 10^{-15} $m^3N^{-1}m^{-1}$ and the average depth of wear track is found as ~1.72 μm, which is less than the thickness of as-deposited coating (~2.2 μm). The width of wear track is found as ~283 μm and the EDX spectrum collected within the wear track shows strong presence of Mo, W and S indicating possible formation of metal sulphides (MoS_2 and WS_2) within the wear track after lubricated sliding. Raman spectrum collected within the wear track of Mo−W−C coating confirms the presence of metal sulphides as shown in Figure 13b. After deconvolution of the spectrum, the D and G graphitic peaks are observed at ~1389.33 cm^{-1} and ~1575.87 cm^{-1} respectively and the I_D/I_G ratio is found as 1.55. Moreover, the peak centred at ~372 cm^{-1} belongs to MoS_2

(Raman peak of MoS_2 powdered sample is observed ~376 cm^{-1}, see Figure 8b) and other deconvoluted peaks are listed in Table 4.

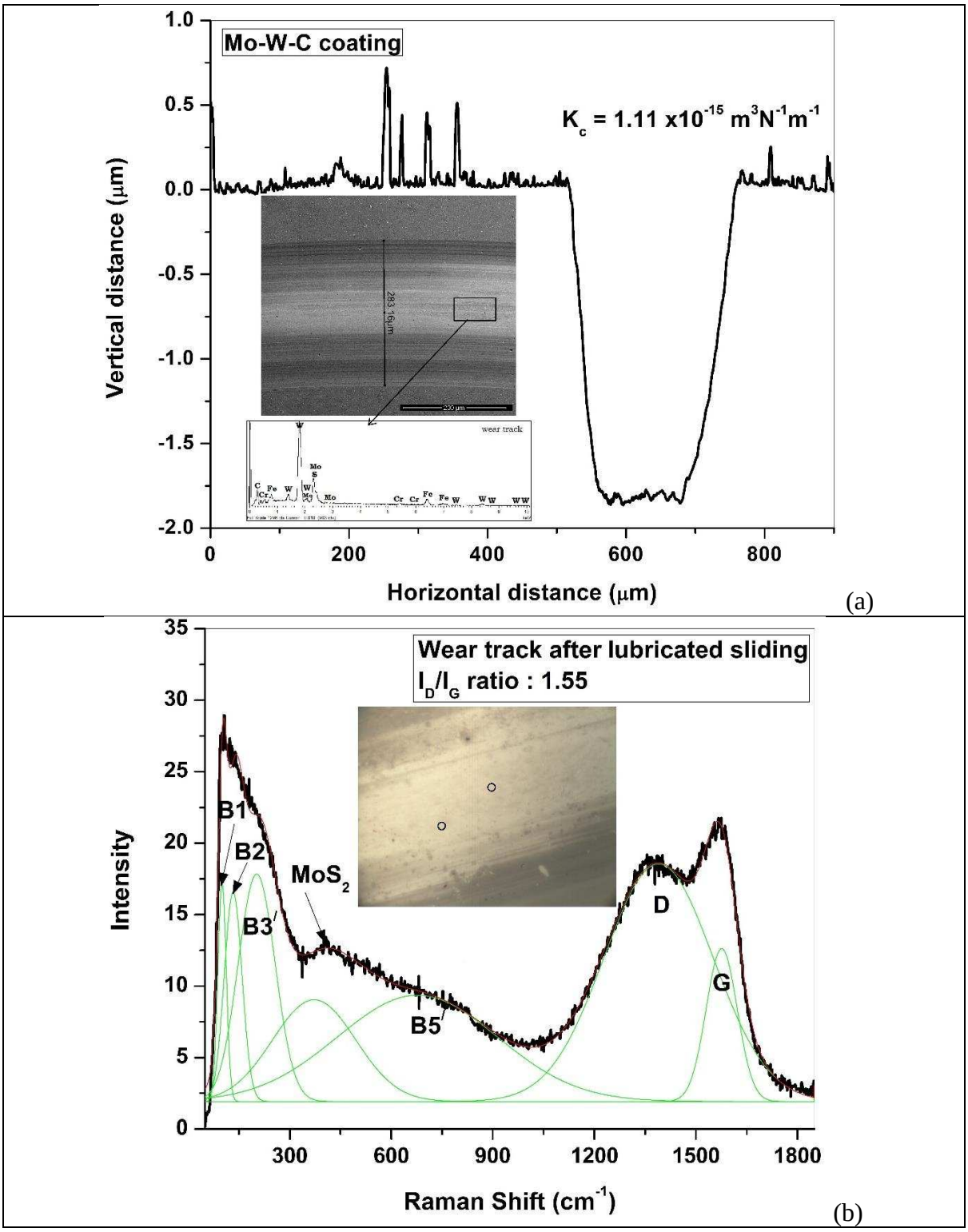

Figure 13: (a) Wear track profile of Mo−W−C coating and the (b) Raman spectrum collected within the wear track after lubricated sliding against steel ball at 200ºC

Table 4: Raman peaks of the spectrum collected from the wear track of Mo−W−C coating after lubricated sliding against steel ball at 200ºC

Raman peaks assigned to the wear track	Raman peaks (this work)	Raman peaks (literature)
B1	~ 100 cm^{-1} with a width of ~ 25 cm^{-1}	–
B2	~ 132 cm^{-1} with a width of ~ 53 cm^{-1}	
$B3^{/}$	~ 202 cm^{-1} with a width of ~ 109 cm^{-1}	
MoS_2	~ 372 cm^{-1} with a width of ~ 245 cm^{-1}	~376 cm^{-1} [figure 4b]
Mo_2C ($B5^{/}$)	~ 677 cm^{-1} with a width of ~ 473 cm^{-1}	~666 cm^{-1} [35]

It should be noted that the as-deposited Mo−W−C coating (I_D/I_G = 1.96) shows higher degree of graphitisation compared to the debris adhered to the steel ball (I_D/I_G = 1.41) and the wear track (I_D/I_G = 1.55) after sliding. The as-deposited coating is graphitic; however the spectra collected from the debris adhered to the steel ball and the wear track show typical D and G peaks, which are similar to those observed in the amorphous carbon coating rather than the graphitic carbon coating. This indicates more disorder of the carbon–carbon bonds of the as-deposited coating after sliding. Due to severe plastic deformation of graphitic debris particles during sliding, the cluster size is significantly decreased and the distortion of the clusters eventually opens up the aromatic rings resulting in a decrease in D peak intensity. This does not affect the relative motion between sp^2 carbon bonds, thus G peak intensity remains same. As a result, I_D/I_G ratio of the as-deposited coating decreases after sliding indicating a possible transformation of nanocrystalline graphitic particles to amorphous phase. Similar to the solid lubricants, these hard amorphous carbon particles decrease the friction.

Figure 14 shows the Raman spectrum collected from the Mo−W−C coated surface beside the wear track after lubricated sliding against steel ball at 200ºC. The oil film was carefully removed from the coated surface before spectrum collection. The D and G graphitic peaks are

observed at ~1384.52 cm^{-1} and ~1574.24 cm^{-1} respectively after deconvolution of the spectrum and the I_D/I_G ratio is found as 1.88. Rest of the deconvoluted peaks are listed in Table 5. Among them, Mo_2C peaks are observed ~338.5 cm^{-1} and ~695 cm^{-1} similar to as-deposited surface and a new Mo_2C peak is appeared ~496 cm^{-1}. As the sample is heated to 200ºC, more amount of Mo_2C is developed and simultaneously amount of free graphitic carbon present in the as-deposited coating is decreased. The formation of Mo_2C in the bulk of the coating at this rather low temperature range has been supported by XRD analyses of the coating after static annealing at 400ºC [38]. The hard Mo_2C phase when abraded against comparatively softer steel counterpart results in simultaneous increase of the friction and wear rate of the counterpart. The abrasion at Mo_2C/steel contacts is seen to be more dominant during the run-in period, (relatively higher coefficient of friction see Figure 10) rather than during the steady-state period when the tribochemically formed lubricious compounds determine the friction and the wear behaviour.

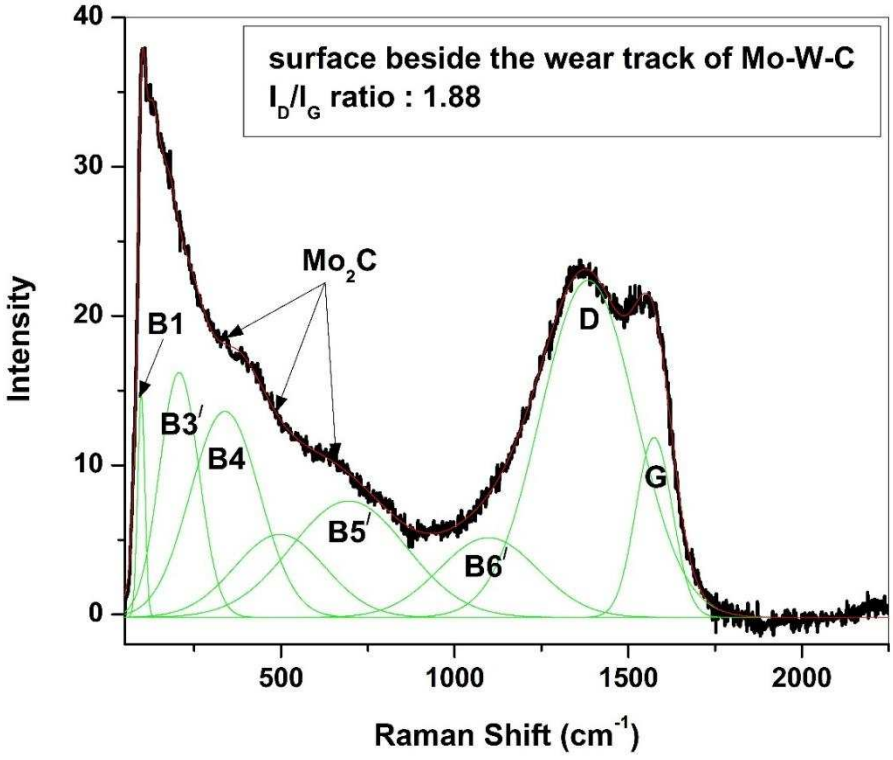

Figure 14: Raman spectrum collected from the Mo−W−C coated surface beside the wear track after lubricated sliding against steel ball at 200ºC

Table 5: Raman peaks of the spectrum collected form the Mo−W−C coated surface beside the wear track after lubricated sliding against steel ball at 200ºC

Raman peaks assigned to the surface beside the track	Raman peaks (this work)	Raman peaks (literature)
B1	~ 97 cm^{-1} with a width of ~ 20.5 cm^{-1}	–
B3/	~ 206 cm^{-1} with a width of ~ 113 cm^{-1}	
Mo_2C (B4)	~ 338.5 cm^{-1} with a width of ~ 200 cm^{-1}	~334 cm^{-1} [35]
Mo_2C	~ 496 cm^{-1} with a width of ~ 260 cm^{-1}	~470 cm^{-1} [35]
Mo_2C (B5/)	~ 695 cm^{-1} with a width of ~ 331 cm^{-1}	~666 cm^{-1} [35]
B6/	~ 1097 cm^{-1} with a width of ~ 283.5 cm^{-1}	–

B. Analyses of the wear behaviour of DLC(Cr/Cr-WC/W:C-H/a:C-H) coating sliding against steel counterpart

Figure 15a shows an SEM image of the wear scar on the counterpart (steel ball) surface and the EDX spectrum collected from this surface before and after lubricated sliding against DLC(Cr/Cr-WC/W:C-H/a:C-H) coating at 200ºC. The spectrum is almost similar to the EDX spectrum collected from the uncoated steel ball before sliding (provided as reference). Both spectra contain Fe, Cr and C peaks, but the absence of S peak indicates no formation of metal sulphides due to tribochemically reactive wear mechanism. This is further confirmed by the Raman analyses of the steel ball after lubricated sliding as shown in

Figure 15b. The spectrum collected from position 1 (worn surface of the steel ball) is found exactly the same to the spectrum collected from uncoated steel ball before sliding whereas the spectrum collected from position 2 (adhered debris on the steel ball) shows presence of distinct disordered and graphitic carbon peaks. After deconvolution of this spectrum, the disordered D1 and D2 peaks are observed at ~1334.55 cm^{-1} and ~1452.24 cm^{-1} respectively

and the G peak is found ~1592.15 cm^{-1}. The I_D/I_G ratio is calculated as ~1.82 indicating graphitic nature of the debris particles. The as-deposited DLC(Cr/Cr-WC/W:C-H/a:C-H) coating is amorphous; therefore the presence of graphitic carbon particles in the debris indicates a structural change of the amorphous particles to graphite-like phase due to severe deformation during sliding.

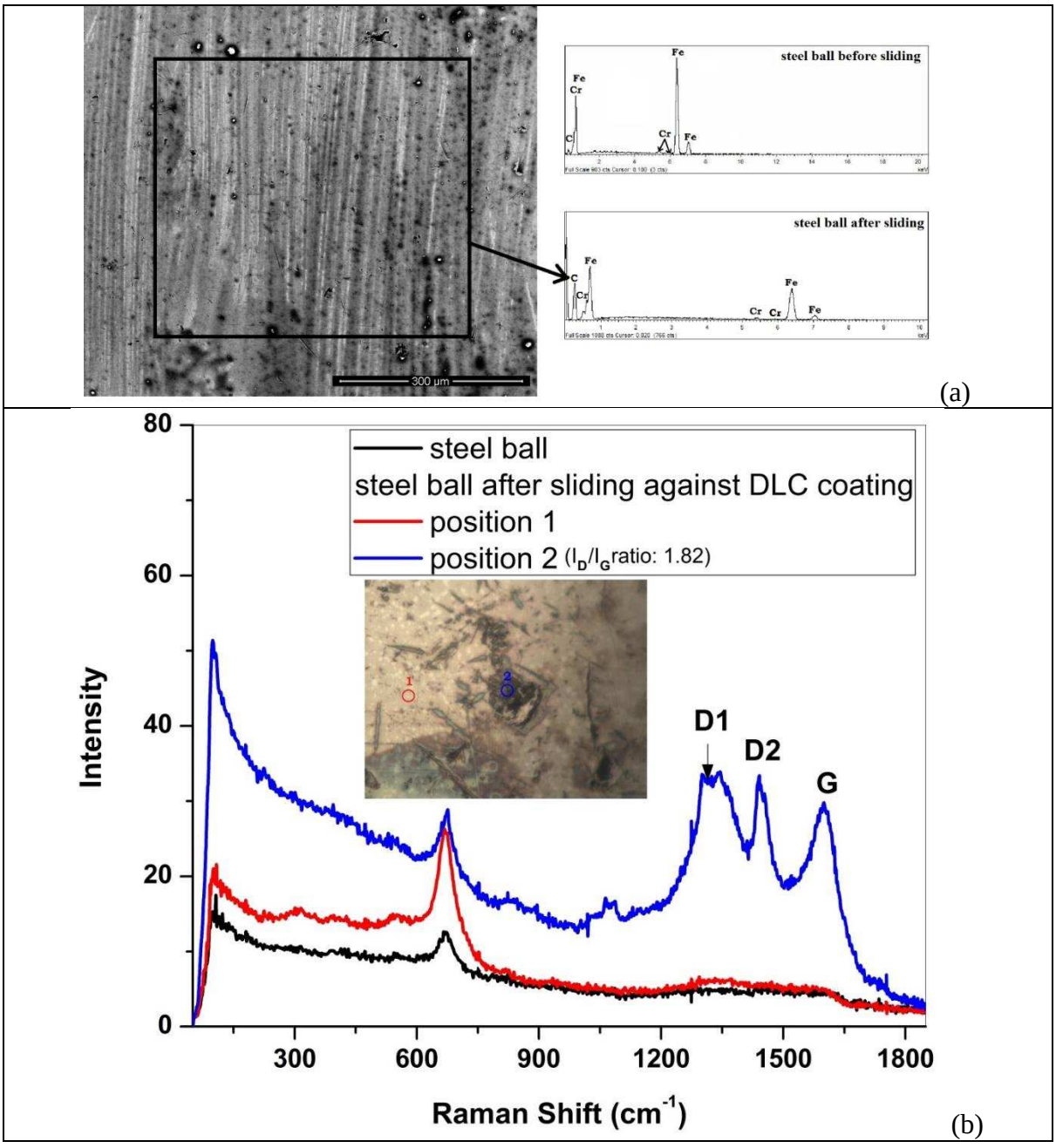

Figure 15: (a) SEM image of the wear scar on the counterpart (steel ball) surface and the EDX spectrum collected from this surface before and after lubricated sliding against

DLC(Cr/Cr-WC/W:C-H/a:C-H) coating at 200ºC. (b) Raman spectra collected from the steel ball after lubricated sliding against DLC(Cr/Cr-WC/W:C-H/a:C-H) coating at 200ºC

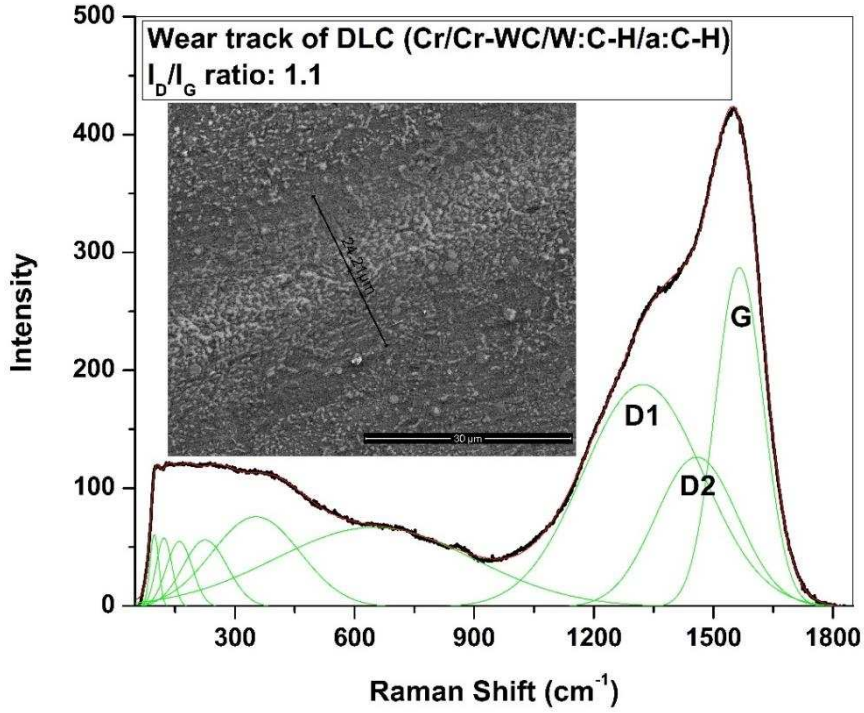

Figure 16 shows the Raman spectrum collected from within the wear track of DLC(Cr/Cr-WC/W:C-H/a:C-H) coating after lubricated sliding at 200ºC. After deconvolution of this spectrum, the disordered D1 and D2 peaks are observed at ~1323.37 cm^{-1} and ~1458.36 cm^{-1} respectively and the G peak is found ~1565.07 cm^{-1}. The development of D peak increases the I_D/I_G ratio to ~1.1. Further it should be noted that the debris adhered to the steel ball (I_D/I_G = 1.82) and the wear track (I_D/I_G = 1.1) have higher degree of graphitisation compared to the as-deposited DLC(Cr/Cr-WC/W:C-H/a:C-H) coating (I_D/I_G = 0.59). The debris particles originated from the coating are severely deformed during sliding, which in turn transforms diamond-like structure of the debris particles into graphite-like structure. As a result, the I_D/I_G ratio increases after sliding compared to the as-deposited coating. The image of the wear track is shown in the inset of

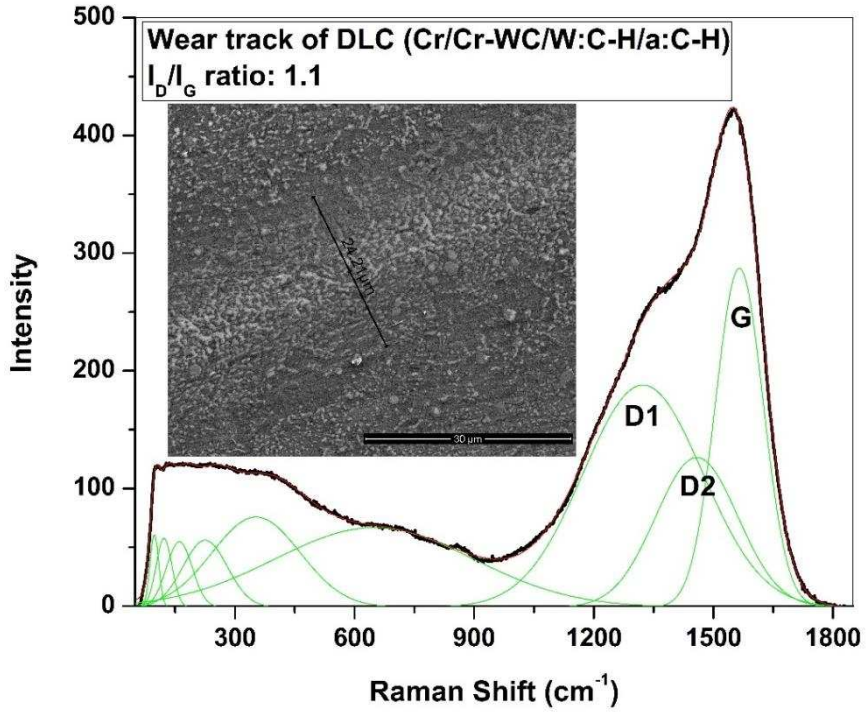

Figure 16. Despite the graphitisation process however, the wear track is very shallow and the wear coefficient is found as low as ~3.06×10^{-18} $m^3N^{-1}m^{-1}$.

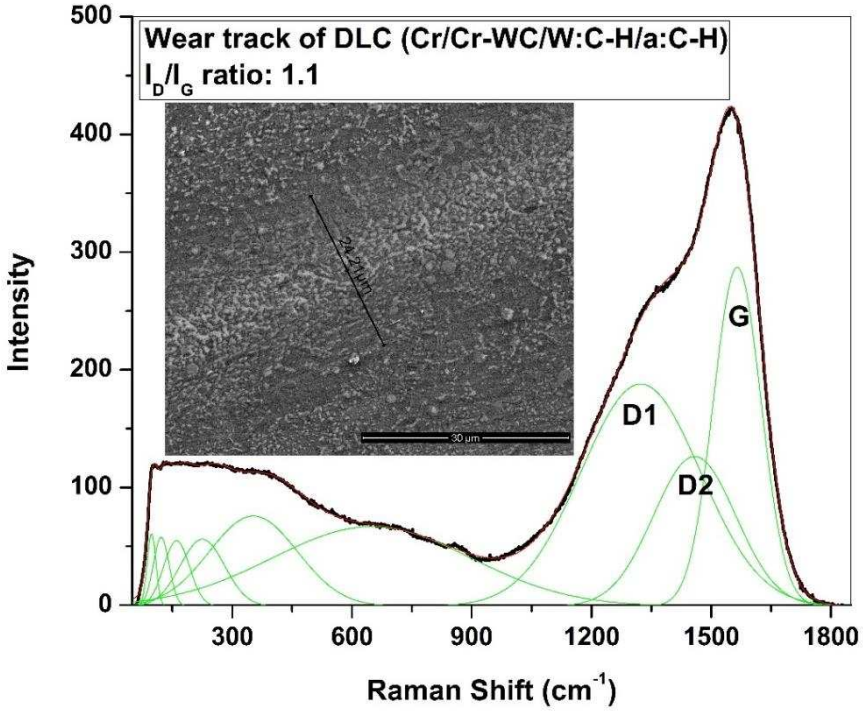

Figure 16: Raman spectrum collected within the wear track of DLC(Cr/Cr-WC/W:C-H/a:C-H) coating after lubricated sliding against steel ball at 200ºC

3.3.2 Friction and wear behaviour *Mo−W−C* and DLC(Cr/Cr-WC/W:C-H/a:C-H) coatings sliding against Al_2O_3 counterpart

Figure 17 shows the friction curves of Mo−W−C and DLC(Cr/Cr-WC/W:C-H/a:C-H) coatings after lubricated sliding against Al_2O_3 counterparts at 200ºC. The friction curve of DLC(Cr/Cr-WC/W:C-H/a:C-H) coating shows almost similar friction in "run-in" period (μ~ 0.083 as in segments I) as well as in "steady-state" period (μ~0.077 as in segment II). Due to the short test duration, no significant degradation of coating properties is observed at 200ºC and therefore almost similar friction coefficient is observed through-out the sliding distance. On the other hand, Mo−W−C coating shows a high friction coefficient in "run-in" period (μ~0.078 as in segment I), followed by a rapid decrease in friction in "steady-state" period (μ~0.038 as in segment II). This reduction in friction is attributed to the formation of low friction transfer layer during lubricated sliding. SEM images and wear track profilometry showed shallow wear tracks for both coatings after sliding against Al_2O_3 balls, see Figure 18. The wear coefficient of DLC(Cr/Cr-WC/W:C-H/a:C-H) however was found to be higher, 6.07 × 10^{-18} $m^3N^{-1}m^{-1}$ compared to negligible (no measurable) wear observed for Mo−W−C coating.

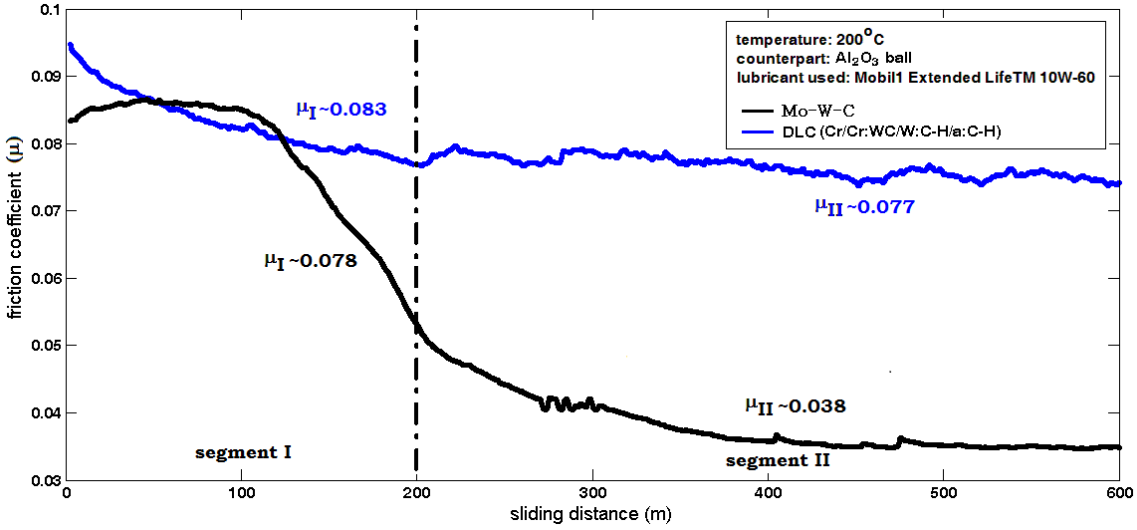

Figure 17: Friction behaviour of Mo−W−C and DLC(Cr/Cr-WC/W:C-H/a:C-H) coatings after lubricated sliding against Al_2O_3 ball at 200ºC

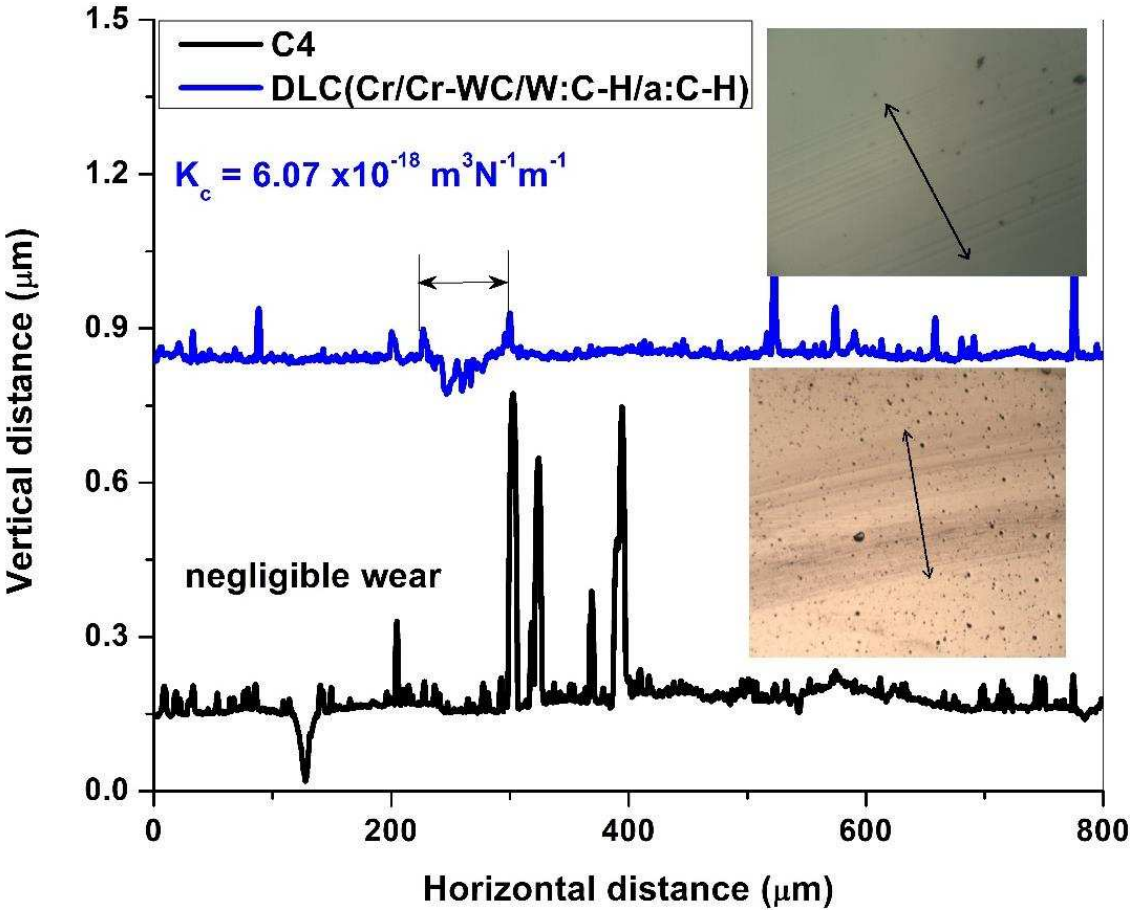

Figure 18: Wear track profiles of Mo−W−C and $\mathrm{DLC}\left(\mathrm{Cr}/\mathrm{Cr}-\mathrm{WC}/\mathrm{W}:\mathrm{C}-\mathrm{H}/\mathrm{a}:\mathrm{C}-\mathrm{H}\right)$ coatings after lubricated sliding against Al_2O_3 counterparts at 200ºC

Raman analysis confirms that the wear debris produced from $\mathrm{DLC}\left(\mathrm{Cr/Cr\text{-}WC/W:C\text{-}H/a:C\text{-}H}\right)$ coating is of amorphous nature (see

Figure 19a). After deconvolution of the spectrum, the disordered D1 and D2 peaks are observed at ~1309.02 cm^{-1} and ~1443.95 cm^{-1} respectively and the G peak is found ~1552.96 cm^{-1}. The I_D/I_G ratio is calculated as ~0.71, which is higher compared to the as-deposited coating (I_D/I_G = 0.59) thus showing the first signs of coating degradation. In contrast, Raman analyses of the wear debris in the wear track of Mo-W-C coatings revealed the presence of graphitic carbon particles but also a considerable amount of the lubricious MoS_2 for providing low friction at elevated temperature.

Figure 19b and

Figure 19c show the Raman spectra collected from two different positions within the wear track of Mo−W−C coating after lubricated sliding. Position 1 shows the spectrum collected from any random position of the wear track (

Figure 19b) and position 2 shows the spectrum collected within the groove formed in the wear track during sliding (

Figure 19c). After deconvolution of the spectrum collected from position 1, the D and G graphitic peaks are observed ~1388.77 cm^{-1} and ~1572.15 cm^{-1} respectively and the I_D/I_G ratio is found ~2.67. The rest of the deconvoluted peaks are found similar to the as-deposited coating (such as B1 − B6′ and Mo_2C) as listed in Table 6. On the other hand, the spectrum collected from position 2 contains two sharp peaks centred at ~371 cm^{-1} and ~405 cm^{-1} respectively along with graphitic carbon peaks. Rest of the deconvoluted peaks (B1 − B6) belong to the as-deposited coating as listed in Table 6. Both sharp peaks belong to MoS_2 phases as the dominant Raman peak of MoS_2 powdered sample is observed ~376 cm^{-1} and ~402 cm^{-1} respectively (see Figure 8b). The D and G peaks are observed ~1394.32 cm^{-1} and ~1569.51 cm^{-1} respectively and the I_D/I_G ratio is found ~2.77. The as-deposited Mo−W−C coating is graphitic (I_D/I_G = 1.96), thus an increase in I_D/I_G ratio (~2.67 at position 1 and ~2.77 at position 2) indicates an increase in disorder of carbon–carbon bonds in the coating after sliding. Therefore low friction and negligible wear of the Mo−W−C coating during lubricated sliding is attributed to the presence of MoS_2 and graphitic carbon particles in the transfer layer.

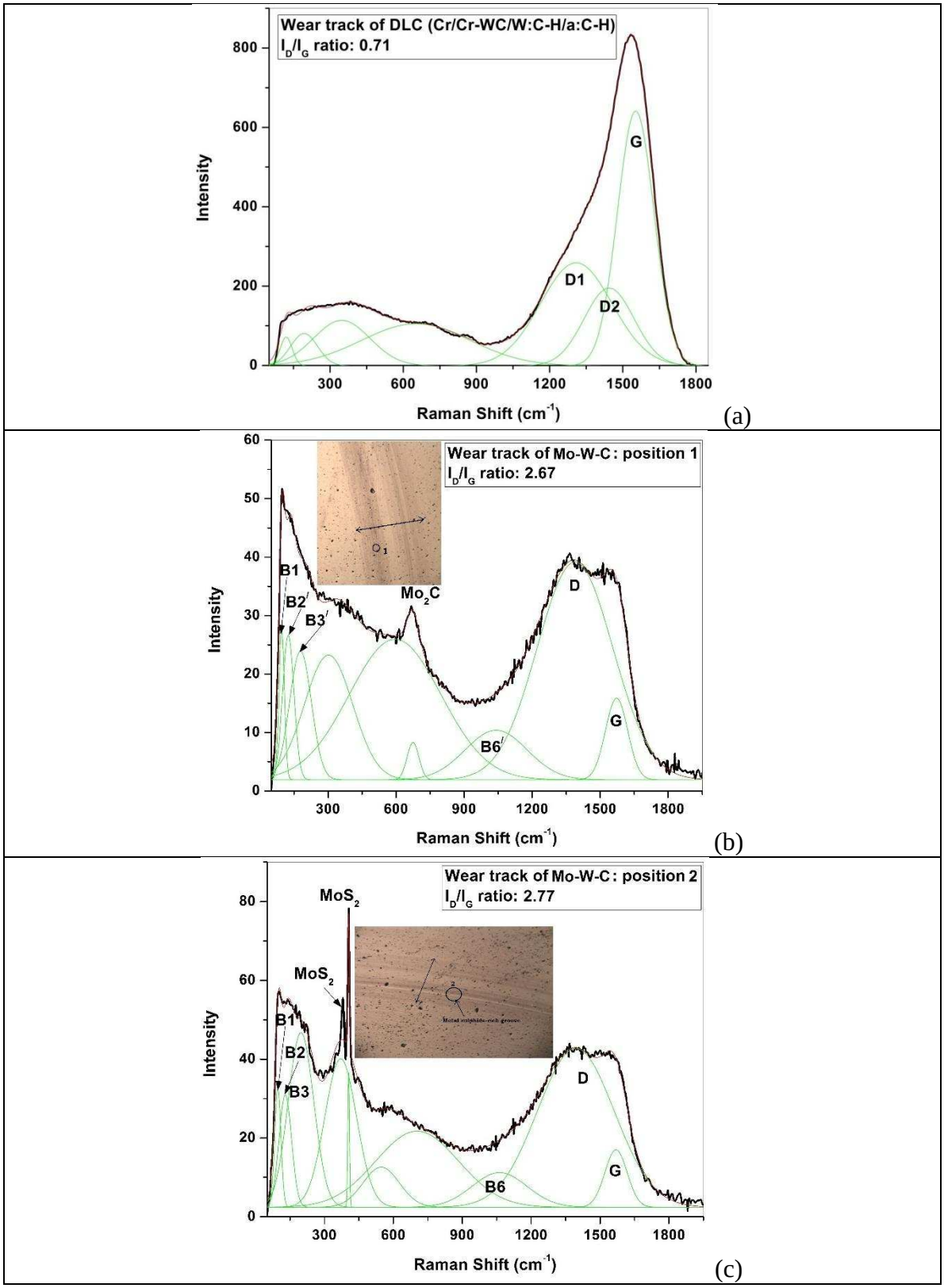

Figure 19: Raman spectra collected within the wear track of (a) DLC(Cr/Cr-WC/W:C-H/a:C-H) and (b – c) Mo−W−C coatings after lubricated sliding against Al_2O_3 ball at 200ºC

Table 6: Raman peaks of the spectra collected from the wear track of C4 after lubricated sliding against Al_2O_3 ball at 200ºC

Raman peaks assigned to the wear track	Raman peaks (this work)	Raman peaks (literature)
(a) wear track: position 1		
B1	~ 95 cm^{-1} with a width of ~ 24 cm^{-1}	–
B2/	~ 124.5 cm^{-1} with a width of ~ 50 cm^{-1}	
B3/	~ 178 cm^{-1} with a width of ~ 96 cm^{-1}	
Mo_2C	~ 674.5 cm^{-1} with a width of ~ 52 cm^{-1}	~666 cm^{-1} [35]
B6/	~ 1041 cm^{-1} with a width of ~ 272 cm^{-1}	–
(b) wear track : position 2		
B1	~ 97 cm^{-1} with a width of ~ 27 cm^{-1}	–
B2	~ 129 cm^{-1} with a width of ~ 55 cm^{-1}	
B3	~ 198 cm^{-1} with a width of ~ 112 cm^{-1}	
MoS_2	~ 371 cm^{-1} with a width of ~ 139 cm^{-1}	~376 cm^{-1} [figure 4b]
MoS_2	~ 405 cm^{-1} with a width of ~ 7.5 cm^{-1}	~402 cm^{-1} [figure 4b]
B6	~ 1062 cm^{-1} with a width of ~ 239 cm^{-1}	–

3.3.3. On the importance of the counterpart material on the wear rate of the *Mo−W−C* coating at elevated temperatures

Our research showed that the wear rate of the Mo-W-C coatings in lubricated sliding is strongly influenced by the counterpart material and the temperature of the surrounding environment. Tribological tests in lubricated sliding at room temperature showed negligible wear of the Mo-W-C independent of the material of the counterpart (steel or Al_2O_3). At elevated temperatures however, the wear coefficient of the coating when sliding against steel ball increased to K_c ~10^{-15} $m^3N^{-1}m^{-1}$. At the same time, the wear of the coating when sliding against Al_2O_3 remained unchanged (negligible), see Figure 18. It was found that when a steel ball is used as sliding counterpart the wear debris generated during sliding tend to adhere

stronger to the counterpart surface and high coating wear is observed. It is believed that the high flash temperatures at the asperity contacts promote metallurgical reactions between the steel and the coating elements such as W, Mo, C. Through diffusion type processes localised at these contact points these reactions can increase the sticking probability of the wear debris to the steel ball counterpart. Increasing the surrounding temperature will further enhance the reaction between the materials involved in the tribo-contact hence the wear rate increase with temperature. It can be speculated that such reaction mechanism will continuously expose new unprotected by tribolayer sliding surface which will result in higher coating wear rates (K_c ~10^{-15} $m^3N^{-1}m^{-1}$). In contrast when the counter part is made of metallurgically inert material such as Al_2O_3, the lubricious wear debris will be sticking more readily to the wear track surfaces thus providing tribological protection and therefore resulting in lower coating wear rates (the coating wear coefficient in this case was negligible).

3.4 Importance of combined Mo and W doping

W-doped DLC coatings are most efficient at low temperatures between ambient [14], [19] and ~100°C [15], [16], [17], [18] combined with lubricated conditions. The tribo-mechanism involves the formation of a WS_2 – containing transfer layer by reactions between the coating and the lubricant, which is highly lubricious. However at higher temperatures, W-doped DLC coatings deteriorate their tribological properties due to decomposition and as a result, enhanced wear of the counterparts was observed [13]. On the other hand it has been reported that Mo-DLC coatings provide low friction at ambient temperature and are most efficient when both phosphorus-based additives and friction modifiers are present in the engine oil. The transfer layer contains a lubricious MoS_2 compound, which is a product of the thermal decomposition of Mo-DTC used as friction modifier [20]. However the decomposition also generates a highly abrasive MoO_3 compound which seriously compromises the performance

of these coatings. Thus it can be concluded that the state of the art carbon coatings doped with only W or Mo are unable to successfully maintain low friction and low wear rate at both ambient and elevated temperature (>100ºC).

Improvement is seen when the carbon coating is simultaneously doped with Mo and W as compared to doping with single metal element. In this work it was shown that Mo−W−C coating provides low friction in boundary lubricated sliding at both ambient as well as elevated temperature (200ºC). Raman analyses revealed that the friction is significantly reduced due to the tribochemically reactive wear mechanism, which forms "in-situ" different solid lubricants such as WS_2 and MoS_2 in the transfer layer depending on the temperature. At ambient temperature, low friction is achieved mostly due to formation of WS_2 and small amount of MoS_2 in the transfer layer. The tribochemical reactions are promoted with increase in test temperature (200^{o}C), which increases the content of MoS_2 in the transfer layer. Thus low friction at elevated temperature is attributed to the presence of both WS_2 and MoS_2. It is important to mention that compared to the case when the friction reduction is achieved by the use of friction modifiers such as Mo-DTC, friction reduction via "in-situ" formation of lubricious phases such as MoS_2 is a more beneficial approach due to the avoidance of the formation of the abrasive MoO_3 compound. In this case the lubricious compound is formed at the asperity contacts where the oxygen supply is effectively hindered, (no formation of abrasive oxides) and present in the sliding spot where it is most needed. Therefore it can be stated that compared to the state of the art single-metal doped carbon coatings the combined Mo and W doped carbon-based coating (Mo−W−C) provides better tribological properties during boundary lubricated sliding at both ambient as well as elevated temperature conditions.

4. Conclusions

Graphitic like Mo- and W- doped Carbon based coatings were successfully produced using the combined HIPIMS and UBM technique. The tribological performance of these coating and commercially available state-of-the-art DLC coatings was compared in boundary lubricated sliding against steel and Al_2O_3 counterpart materials at ambient and elevated (200ºC) temperature conditions. Commercially available engine oil with no friction modifier was used as lubricant). The following conclusions were derived from this study:

- The wear mechanism of Mo−W−C coating at ambient and elevated temperature was found to be tribochemically reactive independent of the counterpart material. High temperatures generated at asperity contacts during lubricated sliding promote tribochemical reactions between the sulphur in the engine oil and the coating elements to form "in-situ" solid lubricants such as WS_2 and MoS_2.
- At ambient temperature during lubricated sliding, the Mo−W−C coating forms a tribolayer containing predominantly graphitic carbon particles, WS_2 and small amount of MoS_2. This low friction tribolayer provides excellent tribological properties ($\mu \sim 0.033$ and negligible wear) compared to a number of state-of-the-art DLC coatings ($\mu \sim 0.043 - 0.092$ and $K_c \sim 10^{-19}\ m^3N^{-1}m^{-1}$).
- At elevated temperature, (200ºC) the formation of lubricious metal sulphides (WS_2 and MoS_2) takes place at higher rate as suggested by the SEM and EDX analyses of the wear track. The tribolayer in this case contains graphitic carbon particles and higher amount of both WS_2 and MoS_2. The presence of the lubricious WS_2 and MoS_2 compounds helps to maintain low values of the coefficient of friction, ($\mu \sim 0.038$). In comparison, when tested under similar conditions state-of-the-art DLC coatings show much higher coefficient of friction ($\mu \sim 0.075 - 0.077$) due to degradation, of coating properties at elevated temperature caused by the graphitisation.

- The wear rate of the Mo-W-C coatings in lubricated sliding at elevated temperatures is strongly influenced by the counterpart material. Higher wear coefficient, Kc was observed when sliding against steel counterpart, ($Kc = 1.11 \times 10^{-15}$ $m^3N^{-1}m^{-1}$) compared to non- measurable wear when the counterpart is made of inert ceramic material such as Al_2O_3. This is attributed to possible metallurgical reactions between coating and counterpart materials which increases the sticking probability of the wear debris to the counterpart thus exposing the worn coating surface unprotected by tribolayer.
- Unlike Mo−W−C coating, no tribochemically reactive wear mechanism was observed for $DLC\left(Cr/Cr\text{-}WC/W\text{:}C\text{-}H/a\text{:}C\text{-}H\right)$ coating at ambient and elevated temperature conditions. Raman analyses confirm no reaction between $DLC\left(Cr/Cr\text{-}WC/W\text{:}C\text{-}H/a\text{:}C\text{-}H\right)$ coating and engine oil during lubricated sliding. Thus the low friction and wear coefficients (μ=0.043 and $K_c \sim 10^{-19}$ $m^3N^{-1}m^{-1}$) of $DLC\left(Cr/Cr\text{-}WC/W\text{:}C\text{-}H/a\text{:}C\text{-}H\right)$ coating were attributed to its extremely high highness (>4300 HV) and the formation of tribolayer containing graphitic particles.

Acknowledgement:

The authors would like to thank IHI Hauzer Techno Coating BV for providing financial support for this research.

Reference:

[1] M Priest and C.M Taylor, “Automobile engine tribology — approaching the surface,” Wear, vol. 241, no. 2, pp. 193-203, 2000.

[2] Y. Liu, A. Erdemir and E.I. Meletis, “An investigation of the relationship between graphitization and frictional behavior of DLC coatings,” Surface and Coatings Technology, Vols. 86-87, pp. 564-568, 1996.

[3] A. Neville, A. Morina, T. Haque and M. Voong, “Compatibility between tribological surfaces and lubricant additives—How friction and wear reduction can be controlled by surface/lube synergies,” Tribology International, vol. 40, p. 1680–1695, 2007.

[4] H. Ronkainen and K. Holmberg, “Environmental and Thermal Effects on the Tribological Performance of DLC coatings,” in Tribology of Diamond-Like Carbon Films, A. E. C. Donnet, Ed., Springer, 2008, pp. 155-196.

[5] Y. Yamamotoa and S. Gondo, “Friction and Wear Characteristics of Molybdenum Dithiocarbamate and Molybdenum Dithiophosphate,” Tribology Transactions, vol. 32, no. 2, pp. 251-257, 1989.

[6] S. Gondo and Y. Yamamoto, “Mechanism of the surface film formation of molybdenum dithiocarbamate (MoDTC) and effect of rubbing materials,” Jpn J Tribol, vol. 36, no. 3, p. 323–333, 1991.

[7] A. Morina, “Lubricant additive interactions, surface reactions and the link to tribological performance in engines (PhD thesis),” Heriot-Watt University, Edinburgh, 2005.

[8] S. Gondo and Y. Yamamoto, “On properties of surface films formed with molybdenum dithiocarbamate (MoDTC) under different conditions,” Jpn J Tribol, vol. 36, no. 3, pp. 309-321, 1991.

[9] T. Haque, A. Morina and A. Neville, “Influence of friction modifier and antiwear additives on the tribological performance,” Surface & Coatings Technology, vol. 204, p. 4001–4011, 2010.

[10] M. d. Barros'Bouchet, J. Martin, T. Le-Mogne and B. Vacher, “Boundary lubrication mechanisms of carbon coatings by MoDTC and ZDDP additives,” Tribology International, vol. 38, pp. 257-264, 2005.

[11] K. Komvopoulos, S. A. Pernama, E. S. Yamaguchi and P. R. Ryason, “Friction Reduction and Anti wear Capacity of Engine Oil Blends Containing Zinc Dialkyl Dithiophosphate and Molybdenum-Complex Additives,” Tribology Transactions, vol. 49, pp. 151-165, 2006.

[12] M. Kalin, E. Roman and J. Vižintin, “The effect of temperature on the tribological mechanisms and reactivity of hydrogenated, amorphous diamond-like carbon coatings under oil-lubricated conditions,” Thin solid films, vol. 515, no. 7-8, pp. 3644-3652, 2007.

[13] B. Podgornik and J. Vižintin, “Tribological reactions between oil additives and DLC

coatings for automotive applications," Surface & coatings technology, vol. 200, no. 5-6, pp. 1982-1989, 2005.

[14] B. Podgornik, S. Jacobson and S. Hogmark, "Influence of EP additive concentration on the tribological behaviour of DLC-coated steel surfaces," Surface & Coatings Technology, vol. 191, p. 357– 366, 2005.

[15] B. Vengudusamy, J. H. Green, G. D. Lamb and H. A. Spikes, "Influence of hydrogen and tungsten concentration on the tribological properties of DLC/DLC contacts with ZDDP," Wear, Vols. 298-299, p. 109–119, 2013.

[16] B. Vengudusamy, J. H. Green, G. D. Lamb and H. A. Spikes, "Tribological properties of tribofilms formed from ZDDP in DLC/DLC and DLC/steel contacts," Tribology international, vol. 44, no. 2, pp. 165-174, 2011.

[17] B. Vengudusamy, J. H. Green, G. D. Lamb and H. A. Spikes, "Behaviour of MoDTC in DLC/DLC and DLC/steel contacts," Tribology international, vol. 54, pp. 68-76, 2012.

[18] L. Yang, A. Neville, A. Brown, P. Ransom and A. Morina, "Friction reduction mechanisms in boundary lubricated W-doped DLC coatings," Tribology internationa, vol. 70, pp. 26-33, 2014.

[19] B. Podgornik, D. Hren and J. ViZintin, "Low-friction behaviour of boundary-lubricated diamond-like carbon coatings containing tungsten," Thin Solid Films, vol. 476, pp. 92-100, 2005.

[20] S. Miyake, T. Saito, Y. Yasuda , Y. Okamoto and M. Kano, "Improvement of boundary lubrication properties of diamond-like carbon (DLC) films due to metal addition," Tribology International, vol. 37, p. 751–761, 2004.

[21] S. Yazawa, I. Minami and B. Prakash, "Reducing Friction and Wear of Tribological Systems through Hybrid Tribofilm Consisting of Coating and Lubricants," Lubricants, vol. 2, pp. 90-112, 2014.

[22] B. Yang, Y. Zheng, B. Zhang, L. Wei and J. Zhang, "The high-temperature tribological properties of Si-DLC films," Surface and Interface Analysis, vol. 44, p. 1601–1605, 2012.

[23] W. J. Wu and M. H. Hon, "Thermal stability of diamond-like carbon films with added silicon," Surface and Coatings Technology, vol. 111, p. 134–140, 1999.

[24] S. C. Jr, A. L. B. Neto, R. A. Santos, F. L. F. Jr, R. Carius and F. Finger, "Improved high-temperature stability of Si incorporated a-C:H films," Diamond and Related Materials, vol. 7, p. 1155–1162, 1998.

[25] R. K.Y. Fu, Y.F. Mei, M. Y. Fu, X. Y. Liu and P. K. Chu, "Thermal stability of metal-doped diamond-like carbon fabricated by dual plasma deposition," Diamond & Related Materials, vol. 14, p. 1489 – 1493, 2005.

[26] A. P. Ehiasarian, J. G. Wen and I. Petrov, "Interface microstructure engineering by high power impulse magnetron sputtering for the enhancement of adhesion," J. Appl. Phys.,

vol. 101, p. 054301, 2007.

[27] A. Ehiasarian, "Fundamentals and Applications of High Power Impulse Magnetron Sputtering," in Plasma Surface Engineering Research and its Practical Applications, Trivandrum, India, Research Signpost, ISBN 978-81, 2007, pp. 35 - 86.

[28] A. P. Ehiasarian, P. E. Hovsepian, L. Hultman and U. Helmersson, "Comparison of microstructure and mechanical properties of chromium nitride-based coatings deposited by high power impulse magnetron sputtering and by the combined steered cathodic arc/unbalanced magnetron technique," Thin Solid Films, vol. 457, p. 270–277, 2004.

[29] P. Mandal, A.P. Ehiasarian and P. Eh. Hovsepian, "Tribological behaviour of Mo − W doped carbon-based coating at ambient condition," Tribology International, vol. 90, p. 135–147, 2015.

[30] "Standard Test Method for Sulfated Ash from Lubricating Oils and Additives, Designation: D 874 – 00," [Online].

[31] "http://www.mobil.co.uk/UK-English-LCW/carengineoils_products_mobil-1-extended-life-10w60.aspx#," [Online].

[32] P. Mandal, A.P. Ehiasarian and P. Eh. Hovsepian, "Lubricated sliding wear mechanism of chromium-doped graphite-like carbon coating," Tribology International, vol. 77, p. 186–195, 2014.

[33] P.Eh. Hovsepian, Y.N. Kok, A.P. Ehiasarian, A. Erdemir, J.G. Wen and I. Petrov, "Structure and tribological behaviour of nanoscale multilayer C/Cr coatings deposited by the combined cathodic arc/unbalnced magnetron sputtering technique," Thin Solid Films, vol. 447, pp. 7-13, 2004.

[34] P.Eh. Hovsepian, Y.N. Kok, A.P. Ehiasarian, R. Haasch, J.G. Wen and I. Petrov, "Phase separation and formation of the self-organised nanostructure in C/Cr coatings in conditions of high ion irradiation," Surface and Coatings Technology, vol. 200, pp. 1572-1579, 2005.

[35] M. L. Frauwallnerr, F. López-Linares, J. Lara-Romero, C. E. Scott, V. Ali, E. Hernández and P. Pereira-Almao, "Toluene hydrogenation at low temperature using a molybdenum carbide catalyst," Applied Catalysis A: General, vol. 394, p. 62–70, 2011.

[36] X. Chen, Z. Peng, Z. Fu, S. Wu, W. Yue and C. Wang, "Microstructural, mechanical and tribological properties of tungsten-gradually doped diamond-like carbon films with functionally graded interlayers," Surface & Coatings Technology, vol. 205, p. 3631–3638.

[37] N. N. Greenwood and A. Earnshaw, "Chapter 23," in Chemistry of the Elements - 2nd edition, Butterworth-Heinemann, 1997.

[38] P. Mandal, A.P. Ehiasarian and P. Eh. Hovsepian, "Isothermal and dynamic oxidation behaviour of Mo − W doped carbon-based coating," Applied Surface Science, vol. 353, p. 1291–1309, 2015.